The diffusion of the atomic metastable particles at 76 °K was found to be described by $D_m p_0 = 146$ cm^2 sec^{-1} Torr. This is to be compared with the value of (163 ± 8) cm^2 sec^{-1} Torr of Ref. 15, which was obtained by using a diffusion cross section of 46×10^{-16} cm^2 ($\pm 5\%$) and Eq. (1) of that work.

The molecular ion He_2^+ was observed to have the same time dependence as He^+. This implies that the conversion of He_2^+ into He_3^+ is much faster than the conversion of He^+ into He_2^+. This finding is consistent with the results of Ref. 2.

The complete behavior of the positive-ion wall currents can be explained in a plausible fashion if one assumes the presence of negative helium ions in the afterglow. On the basis of Ref. 6, the atomic structure of He^-, and the presence of atomic metastable atoms in this work it is likely that the formation of the negative ions involves the atomic and/or molecular metastable particles. No negative ions were detected with the mass filter in the 76 °K afterglow and consequently their presence must be considered as conjectural.

*Work supported by the U.S. Atomic Energy Commission.

[1]M. A. Gusinow, R. A. Gerber, and J. B. Gerardo, Phys. Rev. Letters 25, 1248 (1970).

[2]P. L. Patterson, J. Chem. Phys. 48, 3625 (1968).

[3]R. A. Gerber, M. A. Gusinow, and J. B. Gerardo, Phys. Rev. 3, 1703 (1971).

[4]W. C. Lineberger and L. J. Puckett, Phys. Rev. 186, 116 (1969).

[5]Mark D. Kregel, J. Appl. Phys. 41, 1978 (1970).

[6]B. Brehm, M. A. Gusinow, and J. Hall, Phys. Rev. Letters 19, 737 (1967).

[7]G. N. Estberg and R. W. LaBahn, Phys. Rev. Letters 24, 1265 (1970).

[8]R. A. Gerber, M. A. Gusinow, and J. F. Freeman, Sandia Laboratories Report No. SC-RR-710089 (unpublished).

[9]A. V. Phelps and J. P. Molnar, Phys. Rev. 89, 1202 (1953).

[10]M. A. Gusinow and R. A. Gerber, Phys. Rev. A 2, 1973 (1970).

[11]P. L. Patterson, Phys. Rev. A 2, 1154 (1970).

[12]L. M. Chanin and M. A. Biondi, Phys. Rev. 106, 473 (1957).

[13]A. V. Phelps and S. C. Brown, Phys. Rev. 86, 102 (1952).

[14]B. M. Smirnov, Zh. Eksperim. i Teor. Fiz. 51, 1747 (1966) [Sov. Phys. JETP 24, 1180 (1967)].

[15]W. A. Fitzsimmons, N. F. Lane, and G. K. Walters, Phys. Rev. 174, 193 (1968).

PHYSICAL REVIEW A VOLUME 4, NUMBER 5 NOVEMBER 1971

Intensity-Correlation Spectroscopy*

V. Degiorgio† and J. B. Lastovka‡
Department of Physics and Center for Materials Science and Engineering, Massachusetts Institute of Technology, Cambridge, Massachusetts 02139
(Received 25 March 1971)

In recent years the utilization of "optical mixing" spectroscopic techniques in laser light scattering experiments has proved to be a successful method for the investigation of the dynamical properties of physical systems. By illuminating a photosensitive detector with the scattered light and measuring the spectrum or autocorrelation function of the resulting photocurrent, one can, in general, obtain the ensemble-average time dependence of specific collective excitations within the scattering medium. We present here a detailed quantitative analysis of the statistical errors inherent in such measurements due to the stochastic nature of both the scattering and photoemission processes. We determine the statistical errors on the optical-intensity correlation function as measured by two photocounting digital correlator models and on the intensity spectrum as measured by a "self-beat" optical mixing spectrometer. From these errors and a generalized least-mean-squares fitting procedure we calculate the uncertainty on the measured correlation time (linewidth) for the case of a Gaussian optical field with an exponential intensity correlation function (a Lorentzian spectrum). Scaling relationships are given which permit our numerical results to be applied to an arbitrary set of experimental parameters.

I. INTRODUCTION

In recent years the utilization of "optical mixing" spectroscopic techniques[1,2] in laser light scattering experiments has proved to be a successful method for the investigation of the dynamical properties of physical systems.[3,4] Very generally, the existence of scattering can be attributed to the presence of thermally excited collective and single-particle motions within the scattering medium.[5] Those normal modes of motion which are coupled to the optical dielectric susceptibility of the medium result in index-of-refraction inhomogeneities that are the source of the scattering. By considering the dy-

namics of this scattering process one can show in a straightforward manner that the time behavior of the scattered electric field amplitude mirrors the time evolution of the thermal fluctuation responsible for the scattering. The details of this time evolution can be studied, for example, by measuring the frequency power spectral density of the scattered field $S_E(\omega)$.

In many cases $S_E(\omega)$ extends over a sufficiently large range of frequencies around the laser source frequency ω_0 to allow a determination of the spectrum with conventional grating or Fabry-Pérot spectrometers. These instruments have resolving powers that are typically in the range 10^4–10^8. In numerous situations, however, the desired spectral information is contained in an exceedingly narrow band of frequencies around ω_0, requiring the use of spectroscopic techniques with resolving powers of 10^{10}–10^{15}. Such is the case for the light scattered from concentration fluctuations in binary mixtures[6,7] and macromolecular solutions,[8] entropy fluctuations in normal liquids,[9] density fluctuations in fluids near their critical point,[10,11] surface waves at the interface of single-[12] and two-component[13] fluid systems, and orientation fluctuations in ordered liquid crystals.[14] Optical mixing or light beating spectroscopy provides the only available tool with sufficient spectral resolution to study the dynamics of these fluctuations.

In essence, optical mixing spectroscopy represents an extension of the heterodyne and envelope detection techniques, long familiar at radio frequencies, into the optical-frequency domain. Utilizing the square-law detection characteristic of the photoelectric effect, one can observe in the photocurrent signal the beating between two closely spaced optical frequencies or recover the slowly varying envelope of a rapidly oscillating optical field. The net result is a translation of the optical spectral information centered around the frequency $\omega_0 \approx 5\times10^{14}$ Hz to a current spectrum at frequencies near $\omega = 0$, where a resolution of 1 Hz is easily achieved.

Since the current output of a photoelectric device is proportional to the instantaneous optical intensity I, the current provides a signal from which we may determine the *intensity* power spectrum $S_I(\omega)$ or equivalently the *intensity* autocorrelation function $R_I(t)$. With respect to a light scattering experiment, one can show that a measurement of $S_I(\omega)$ or $R_I(t)$ usually contains the desired information on the time evolution of the fluctuation which gave rise to the scattering.[4,10,15] Moreover, $S_I(\omega)$ or $R_I(t)$ are also useful quantities for characterizing the time behavior of the fields emitted by light sources such as a laser[16,17] or a quasithermal blackbody radiator.[18,19]

Many different electronic techniques have been used to extract various features of the correlation function or the spectrum of the photocurrent signal, such as analog[13,20] and digital correlators,[7,19,21] joint-photocount distributions,[22] arrival-time-interval photocount distributions,[23] single-interval photocount distributions,[24] and optical mixing spectrometers.[1,8–10,16] Since the photocurrent autocorrelation function $R_i(t)$ and the photocurrent power spectral density $S_i(\omega)$ are simply Fourier-transform pairs, all these methods, in principle, give equivalent information. From a practical point of view, however, one would like to achieve the highest possible measurement accuracy in the minimum amount of time. The ultimate limit to the precision of these measurements is determined by statistical errors due to the finite measurement time. Therefore we shall try in this paper to answer the following question: How large is the statistical error on a measurement of $S_i(\omega)$ or $R_i(t)$, given the measurement time, the properties of the incident optical field, and the measuring device? In particular, we will consider an incoming optical field with Gaussian amplitude statistics and an exponential intensity correlation function (a Lorentzian spectrum), and we calculate the statistical errors (a) on the photocurrent correlation function $R_i(t)$ for an arbitrary delay t, (b) on the correlation time τ_c, (c) on the photocurrent spectrum $S_i(\omega)$, and (d) on the Lorentzian half-width of the spectrum Γ. In the process we also determine "optimum" values for each of the free experimental parameters, optimum in the sense that they minimize the statistical errors in each case.

The literature on this subject is not very rich. There has been some treatment of the errors in the ensemble-average (time-independent) photocount distribution, both for correlated and uncorrelated samples[25]; signal-to-noise analyses of optical mixing spectrometers[4,15,26]; and error treatments of correlation function measurements on continuous Gaussian variables.[27] Haus[28] was the first to outline a detailed treatment of the type we present here; however, he did not study the problem of the errors on the correlation time (or the linewidth of the spectrum) which, we believe, is the most significant way of discussing the relevant statistical errors.

The organization of our paper is as follows: In Sec. II we recall some useful relations regarding photocount distributions and correlation functions; in Sec. III we calculate an expression for the statistical errors on the photocurrent autocorrelation function and specialize our results to a particular model of an "ideal" digital correlator; in Sec. IV we apply the general method of Sec. III to the case of a "clipped correlator"; in Sec. V we evaluate the statistical error on the correlation time by considering a generalized least-mean-square-error fitting procedure; in Sec. VI we evaluate the statis-

tical errors on the photocurrent spectrum and its linewidth as measured by a "self-beating" optical mixing spectrometer; in Sec. VII we determine the effect of collecting light from an arbitrary number of spatial coherence areas of the optical field; in Sec. VIII we summarize the numerical results obtained and make a critical evaluation of the various techniques used to process the photocurrent signal.

II. REVIEW OF PROPERTIES OF PHOTOCOUNT DISTRIBUTION FUNCTIONS

We want to recall here some useful definitions and results regarding photocounting distributions and correlation functions.[29] The definition of the general optical field intensity correlation function $\mathcal{G}^{(n)}$ of order n is

$$\mathcal{G}^{(n)}=\langle E^{(-)}(X_1)\cdots E^{(-)}(X_n)E^{(+)}(X_n)\cdots E^{(+)}(X_1)\rangle\ , \tag{1}$$

where $E^{(-)}$ and $E^{(+)}$ are, respectively, the electric field operators corresponding to negative and positive frequencies and the $X_1,\ldots,X_n=(\vec{r}_n,\ t_n)$ indicate n space-time positions. The angle brackets denote an ensemble average which can be performed once the density matrix for the field is known. In particular, $\mathcal{G}^{(1)}$ is simply the average intensity of the field and $\mathcal{G}^{(2)}$ is the usual two-point intensity correlation function.

The corresponding two-point correlation function measured in a photocounting experiment is

$$\begin{aligned}G^{(2)}(X_1,\ X_2)\Delta X_1\Delta X_2&\\ =\sum_{n_1=1}^{\infty}\sum_{n_2=1}^{\infty}&n_1n_2W_2(n_1,\ X_1,\ \Delta X_1;\ n_2,\ X_2,\ \Delta X_2)\\ \equiv\langle n_1(X_1,\ \Delta X_1)&n_2(X_2,\ \Delta X_2)\rangle\ ,\end{aligned} \tag{2}$$

where W_2 is the joint probability of observing n_1 counts at X_1 in the space-time interval ΔX_1 and n_2 counts at X_2 in the interval ΔX_2.[22] Since the instantaneous probability of a photoemission event at X_n is proportional to the field intensity at X_n, W_2 is related to $\mathcal{G}^{(2)}$ as follows:

$$\begin{aligned}W_2(1,\ X_1,\ \Delta X_1;\ 1,\ X_2,\ \Delta X_2)&\\ =(\epsilon^2c/8\pi)\,\mathcal{G}^{(2)}(X_1,\ X_2)\Delta X_1\Delta X_2\ .&\end{aligned} \tag{3}$$

In Eq. (3), c is the velocity of light and ϵ is the quantum efficiency of the photodetector. Although the higher-order photocount correlation functions $G^{(n)}(X_1,\ldots,X_n)$ contain additional information[30] on the time evolution of the incoming field, we restrict our attention in this paper to measurements of $G^{(2)}$. Further we shall consider here only the time dependence of $G^{(2)}$. For a stationary field, $G^{(2)}$ will be a function only of the time difference $t=|t_2-t_1|$, and we write $G^{(2)}(X_1,\ X_2)=G^{(2)}(t)$.

The qualitative features of $G^{(2)}(t)$ may be elucidated as follows. In the limit $t\to\infty$, the photoevents at t_1 and t_2 are uncorrelated and Eq. (2) becomes

$$\lim_{t\to0}G^{(2)}(t)(\Delta t)^2=\sum_{n_1=1}^{\infty}\sum_{n_2=1}^{\infty}n_1n_2W_1(n_1,\ \Delta t)W_1(n_2,\ \Delta t)\ , \tag{4}$$

where $W_1(n,\ \Delta t)$ is the simple probability of having n counts in the interval $\Delta t=\Delta t_1=\Delta t_2$. We find then

$$\lim_{t\to\infty}G^{(2)}(t)(\Delta t)^2=\langle n\rangle^2\ , \tag{5}$$

independent of t, where $\langle n\rangle$ is the average number of photocounts per Δt. Clearly $G^{(2)}(\infty)$ represents the contribution of the average dc photocurrent to the current correlation function.

In the opposite limit $t\to0$ we must be more careful. Consider first the case $t\equiv0$ *and* $\Delta t_1=\Delta t_2=\Delta t\to0$ where $n=n_1=n_2$ will take on only the values of 0 or 1. Then we find

$$\begin{aligned}\lim_{\Delta t\to0}G^{(2)}(0)(\Delta t)^2\equiv G_s^{(2)}(0)(\Delta t)^2&=(1)(1)W_1(1,\ \Delta t)\\ &=\langle n\rangle=\eta\Delta t\ ,\end{aligned} \tag{6}$$

where $G_s^{(2)}(0)$ represents the self-correlation of individual photoevents and η is the average photoelectron counting rate. Rewriting $G_s^{(2)}(0)$ in the form

$$G_s^{(2)}(0)\Delta t=\int_{-\Delta t/2}^{\Delta t/2}G_s^{(2)}(t)\,dt\ , \tag{7}$$

we find $G_s^{(2)}(t)=\eta\delta(t)$ with $\delta(t)$ being the Dirac delta function. $G_s^{(2)}(t)$ is the photoelectron "shot-noise" part of $G^{(2)}(0)$. Taking the limit $t\to0$ with $\Delta t\neq0$ gives from Eq. (2)

$$\lim_{t\to0}G^{(2)}(0)=\sum_{n=1}^{\infty}n^2W_1(n,\ \Delta t)=\langle n^2\rangle\ . \tag{8}$$

From Eqs. (5), (6), and (8) we can construct the general features of $G^{(2)}(t)$ shown in Fig. 1: a shot-noise δ function at $t=0$, a constant background term related to the time-average photocurrent, and a "signal" term which, via Eq. (3), reproduces the time-delay dependence of the optical intensity correlation function $\mathcal{G}^{(2)}$.

In order to calculate the error on a measurement of $G^{(2)}(t)$ we will need various moments of the counting distribution functions. We now summarize briefly the relevant definitions.

Given the probability distribution $W_1(n)$ one can define the moment of Kth order, M_K, as

$$M_K=\sum_{n=0}^{\infty}n^KW_1(n)=\langle n^K\rangle \tag{9}$$

and the factorial moment F_K as

$$\begin{aligned}F_K=\sum_{n=0}^{\infty}&n(n-1)\cdots(n-K+1)W_1(n)\\ &=\langle n(n-1)\cdots(n-K+1)\rangle\cdot\end{aligned} \tag{10}$$

The generalization of Eqs. (9) and (10) to the case

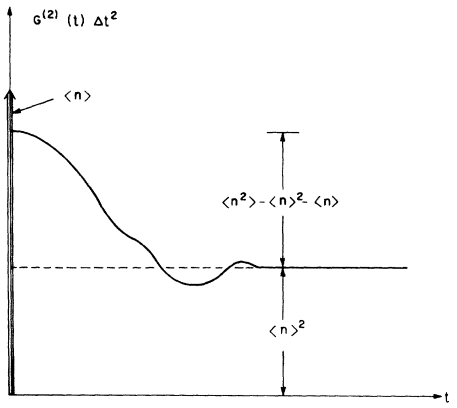

FIG. 1. General features of the photocount autocorrelation function.

of the m-time joint probability distribution W_m is straightforward; we define

$$M_{K_1,K_2,\ldots,K_m} = \langle n_1^{K_1} \cdots n_m^{K_m} \rangle \tag{11}$$

and

$$F_{K_1,K_2,\ldots,K_m} = \langle [n_1(n_1-1)\cdots(n_1-K_1+1)]\cdots \times [n_m(n_m-1)\cdots(n_m-K_m+1)]\rangle . \tag{12}$$

It is easy to recognize from Eq. (2) that $G^{(2)} = M_{11} = F_{11}$ and from Eqs. (5), (6), and (8) that excluding the shot-noise term, $G^{(2)}(0) = F_2$. The generalized moments in Eqs. (11) and (12) can be more easily evaluated from a generating function Q_m than from the joint probability W_m.[22,31] The definition of Q_m is

$$Q_m(s_1, s_2, \ldots, s_m) = \sum_{n_1=0}^{\infty} \cdots \sum_{n_m=0}^{\infty} [(1-s_1)^{n_1}\cdots(1-s_m)^{n_m}] W_m(n_1 \cdots n_m) = \langle (1-s_1)^{n_1}\cdots(1-s_m)^{n_m}\rangle . \tag{13}$$

Using this definition it is easy to show that

$$F_{K_1\cdots K_m} = (-1)^{K_1+K_2+\cdots K_m} \frac{\partial^{K_1}}{\partial s_1^{K_1}} \cdots \frac{\partial^{K_m}}{\partial s_m^{K_m}} Q_m \times (s_1, \ldots, s_m)\big|_{s_1=\cdots s_m=0} . \tag{14}$$

Therefore knowing Q_m one can obtain all the corresponding factorial moments by differentiation; the moments $M_{K_1\cdots K_m}$ can then be evaluated using the relationships between M and F derivable from the definitions given in Eqs. (11) and (12).

III. STATISTICAL ERRORS IN MEASUREMENT OF CORRELATION FUNCTION

We now proceed to calculate the unavoidable statistical error in a measurement of the photocurrent correlation function due to a finite measuring time, or equivalently, to a finite number of recorded photocounts. There can be many other sources of "noise" in a measurement of $G^{(2)}(t)$, e.g., amplitude instability of the light source in a scattering experiment, the presence of stray light, detector dark current, etc. The importance of these effects will vary from one experiment to another; therefore, it is difficult to take them into account in a general treatment. Usually, however, one can vary the experimental parameters in such a way that these extraneous noise contributions play a negligible role.

We first discuss an "ideal" digital correlation experiment: (i) A photomultiplier is illuminated with a "single-mode" electromagnetic field. In a light scattering experiment, single mode implies that the detector collection area is smaller than a single spatial coherence area[2,4,26] of the scattered field; (ii) we assume that the light intensity is small enough so that it is possible to time-resolve single photoelectron pulses at the output of the photodetector; (iii) the output pulses are amplitude and shape standarized in order to get rid of the statistics of the single electron response of the photomultiplier. This operation introduces a dead time in the measurement; hence, we use the assumption that the photoelectron counting rate is small in order to neglect dead-time losses[32]; (iv) we will discuss intensity correlation times τ_c which are much longer than the natural rise time of the photodetector, τ_r. A measurement of the correlation function is still possible for $\tau_c \leq \tau_r$, but the interpretation of the result and the measurement technique are different from the situation we consider here; (v) we arrange to record the sequence of photoelectron pulses for a total time T. This record is then subdivided into M_0 equal intervals each of length Δt. For each $t_j = j\Delta t$ we determine the number of counts n_j recorded between t_j and $t_j + \delta t$ where $\delta t \leq \Delta t$. The experimental value of the current autocorrelation function for a delay $t = l\Delta t$ is then calculated as

$$R_l = \frac{1}{M_0} \sum_{j=1}^{M_0} n_j n_{j+l} , \tag{15}$$

where n_j and n_{j+l} are, respectively, the number of counts collected at times $j\Delta t$ and $(j+l)\Delta t$ in an interval δt. If we define $\bar{R}_l$ as the "true" correlation function, that is the limit of R_l as T becomes infinite, the ensemble-average mean-square-error on R_l will be

$$\langle \delta R_l^2 \rangle = \langle (R_l - \bar{R}_l)^2 \rangle = \frac{1}{M_0^2} \sum_{j=1}^{M_0} \sum_{k=1}^{M_0} \langle n_j n_{j+l} n_k n_{k+l} \rangle - \bar{R}_l^2 . \tag{16}$$

That is $\langle \delta R_l^2 \rangle$ gives the variance of R_l as evaluated on an ensemble of identical experiments each lasting for a time T.[33] Equivalently, one can say that $\langle \delta R_l^2 \rangle^{1/2}$ is an error band around $\bar{R}_l$ which gives the mean probable deviation between any single measurement of R_l and its true ensemble-average value.

Let us now introduce the separation s between the starting times of two samples:

$$s = |j - k| \ . \tag{17}$$

In terms of the positive integer s and the generalized moments defined in Eqs. (11) and (12) we can rewrite Eq. (16) in the form

$$\langle \delta R_l^2 \rangle = \frac{M_{22}(0, l)}{M_0} + \frac{2(M_0 - l)}{M_0^2} M_{121}(0, l, 2l) + \frac{2}{M_0^2} \sum_{s=1, s\neq l}^{M_0} (M_0 - s) M_{1111}(0, l, s, s+l) - M_{11}^2(0, l) \ . \tag{18}$$

It is important to note two subtle features of Eqs. (15) and (18). In the limit $l \equiv 0$ our ideal correlator model gives $R_0 = \langle n^2 \rangle$ rather than the sum of the "signal" and "dc" parts of $G^{(2)}(t)$, namely, $\langle n(n-1) \rangle$ However $\langle \delta R_l^2 \rangle$ as given in Eq. (18) represents the error on the quantity $\langle n(n-1) \rangle$ if $l = 0$. Therefore $\langle \delta R_0^2 \rangle$ is strictly speaking the limit

$$\langle \delta R_0^2 \rangle = \lim_{l \to 0, l \neq 0} \langle \delta R_l^2 \rangle \tag{19}$$

and does not include the error on the shot-noise δ-function part of R_l at $l = 0$.

Equation (18) is valid for an arbitrary incident optical field. To proceed further we need explicit assumptions concerning the statistics and intensity correlation function of this field. We choose here the situation most frequently encountered in practice, namely, a Gaussian field with a simple decaying exponential intensity correlation function. For such a Gaussian field the ensemble-average distribution W_1 for the number of photocounts collected in an interval $\delta t \ll \tau_c$ is the Bose-Einstein distribution

$$W_1(n, \delta t) = \langle n \rangle^n / (1 + \langle n \rangle)^{n+1} \ . \tag{20}$$

The ensemble-average correlation function $\bar{R}_l = G^{(2)}(l \Delta t)$ is

$$\bar{R}_l = M_{11}(0, l) = \langle n \rangle^2 (1 + e^{-l \Delta t / \tau_c}) \ , \tag{21}$$

where τ_c is the correlation time of the field-intensity correlation function. The required higher-order moments M_{22}, M_{121}, M_{1111} can now be computed using the two-, three-, and four-dimensional generating functions Q_2, Q_3, Q_4 which have been calculated by Arecchi, Berné, and Sona[22] and by Bédard[31] for the type of optical field we are considering. The results are

$$\begin{aligned} M_{22}(0, l) &= 4\langle n \rangle^4 (1 + 4e^{-l \Delta t / \tau_c} + e^{2l \Delta t / \tau_c}) \\ &\quad + 4\langle n \rangle^3 (1 + 2e^{-l \Delta t / \tau_c}) + \langle n \rangle^2 (1 + e^{-l \Delta t / \tau_c}) \ , \\ M_{121}(0, l, 2l) &= 2\langle n \rangle^4 (1 + 4e^{-l \Delta t / \tau_c} + 7e^{-2l \Delta t / \tau_c}) \\ &\quad + \langle n \rangle^3 (1 + 2e^{-l \Delta t / \tau_c} + 3e^{-2l \Delta t / \tau_c}) \ , \\ M_{1111}(0, l, s, s+l) &= \langle n \rangle^4 (1 + 2e^{-l \Delta t / \tau_c} + 6e^{l s \Delta t / \tau_c} \\ &\quad + e^{-2l \Delta t / \tau_c} + 4e^{-2s \Delta t / \tau_c} \\ &\quad + 9e^{-(s+l) \Delta t / \tau_c} + e^{-(s-l) \Delta t / \tau_c}) \ . \end{aligned} \tag{22}$$

The expression given for M_{1111} is appropriate for $s > l$; for $s < l$ the correct result is obtained by interchanging s and l. Substituting the results in Eqs. (21) and (22) into Eq. (18) and performing the sum over s, we obtain

$$\begin{aligned} \langle \delta R_l^2 \rangle = \frac{\langle n \rangle^4}{M_0} \Bigg[&-5 + \frac{8}{1 - e^{-\Delta t / \tau_c}} + \frac{2}{1 - e^{-2\Delta t / \tau_c}} \\ &+ 4\left(2l - 3 + \frac{6}{1 - e^{-\Delta t / \tau_c}}\right) e^{-l \Delta t / \tau_c} \\ &+ 3\left(2l - 1 + \frac{2}{1 - e^{-2\Delta t / \tau_c}}\right) e^{-2l \Delta t / \tau_c} \Bigg] \\ &+ \frac{6\langle n \rangle^3}{M_0} (1 + 2e^{-l \Delta t / \tau_c} + e^{-2l \Delta t / \tau_c}) \\ &+ \frac{\langle n \rangle^2}{M_0} (1 + e^{-l \Delta t / \tau_c}) \ . \end{aligned} \tag{23}$$

The approximation $M_0 \gg l$ has been used in order to simplify Eq. (23). This condition will be satisfied under all usual experimental conditions.

Equation (23) represents the result we will use in Sec. IV to evaluate the statistical error on the measured correlation time. However an important preliminary estimate of the precision of the measurement of R_l is the ratio

$$\Delta_R \equiv \langle \delta R_0^2 \rangle^{1/2} / \langle n \rangle^2 \ , \tag{24}$$

where $\langle n \rangle^2 = \langle n^2 \rangle - \langle n \rangle^2 - \langle n \rangle$ is the amplitude of the exponential (signal) part of R_0.[34] The ratio Δ_R gives the root-mean-square uncertainty in R_0 as a fraction of this signal amplitude.

Figure 2 shows the behavior of Δ_R as a function of $\langle n \rangle$ calculated with $T = 10$ sec, $\tau_c = 10^{-3}$ sec, and $\delta t = \Delta t = 0.05\tau_c$. For a fixed counting rate per second η, the value of $\langle n \rangle$ depends only on the gate interval width, δt; the upper abscissa in Fig. 2 gives the number of counts per correlation time, $\eta\tau_c$, corresponding to our choice for δt. The asymptotic behavior of Δ_R in the two limits $\langle n \rangle \to 0$ and $\langle n \rangle \to \infty$ can be evaluated simply from Eq. (23). For large $\langle n \rangle$ we find $\langle \delta R_l^2 \rangle \propto \langle n \rangle^4$; therefore, Δ_R becomes independent of $\langle n \rangle$. We see from Fig. 2 that this asymptotic limit is already well established when $\langle n \rangle \cong 1$. More explicitly, for large $\langle n \rangle$ and small $\Delta t / \tau_c$ we find

$$\Delta_R \cong 6(\tau_c / T)^{1/2} \ , \quad \langle n \rangle \to \infty \tag{25}$$

where we note that (T/τ_c) is an intuitive estimate of the number of statistically independent samples of R_l which can be obtained in a time T. A confirmation of this interpretation can be obtained from a calculation of Δ_R for a set of M truly statistically independent samples of R_0 which we find, in the

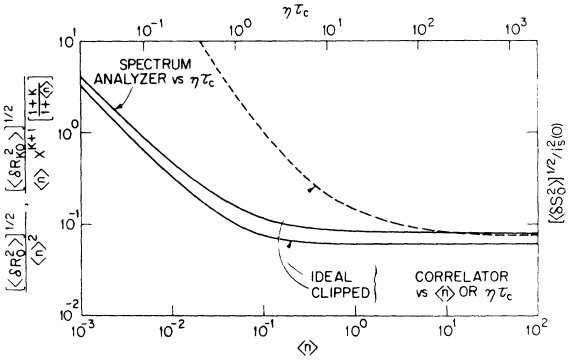

FIG. 2. rms fractional errors Δ_R, Δ_K, and Δ_S versus counting rate. A discussion of the numerical parameters used to obtain these results can be found in the text.

limit $\langle n\rangle \to \infty$,

$$\Delta_R^* = (20/M)^{1/2}, \quad \langle n\rangle \to \infty \tag{26}$$

independent of $\langle n\rangle$. Comparing Eqs. (25) and (26) indicates that our model correlator obtains an "independent sample" of R_0 every $1.8\tau_c$.

For small $\langle n\rangle$ we have $\langle \delta R_i^2\rangle = \langle n\rangle^2/M_0$ and

$$\Delta_R = \left(\frac{2\Delta t}{T}\right)^{1/2}\frac{1}{\langle n\rangle}, \quad \langle n\rangle \to 0 . \tag{27}$$

Again this result can be compared to the result for M statistically independent samples, which is

$$\Delta_R^* = \left(\frac{2}{M}\right)^{1/2}\frac{1}{\langle n\rangle}, \quad \langle n\rangle \to 0 . \tag{28}$$

In this limit we see that all of our $M_0 = T/\Delta t$ samples can be considered independent. This is not surprising when the counting rate becomes less than one count per correlation time. It is perhaps useful to point out that *both* limiting expressions for the fractional error have the required form of "the square root of one over the number of statistically independent samples." Equation (25) is clearly of this form; Eq. (28) is also if we note that for $\langle n\rangle \ll 1$ only $M_0\langle n\rangle^2$ samples out of a total of M_0 samples are different from zero and therefore contain any information.

Although the numerical results presented in Fig. 2 have been calculated for a specific set of experimental parameters, i.e., $T = 10.0$ sec, $\tau_c = 10^{-3}$ sec, and $\Delta t/\tau_c = 0.05$, they can be used to obtain Δ_R for arbitrary values of these parameters by relocating the asymptotic features via Eqs. (25) and (27).

IV. CLIPPED DISTRIBUTIONS

We now repeat the computation made in Sec. III for the case in which the photocount signal is "clipped" during the measurement of $G^{(2)}(t)$. Introducing a positive integer clipping level K for the number of counts collected in the interval δt, we define the clipped count as

$$n^{(K)} = \begin{cases} 1, & n > K \\ 0, & n \le K . \end{cases} \tag{29}$$

The correlation function we discuss here is $R_K(t) = \langle n^{(K)}(0)\, n(t)\rangle$; that is, we consider a situation in which clipping is performed only on the initial member of a pair of samples of n. Our interest in this particular clipped correlation function lies in the fact that a device that measures $R_K(t)$ over a wide range of delay times can readily be constructed using commercial apparatus.

Correlation of clipped signals was first discussed by Van Vleck[35]; Jakeman and Pike[36] were the first to consider clipping as applied to photocount signals. The latter authors have performed an explicit computation for the photocount correlation function $\bar{R}_K$ assuming a Gaussian optical field with exponential intensity correlation function; their result is

$$\bar{R}_K(t) = \langle n\rangle\left(\frac{\langle n\rangle}{1+\langle n\rangle}\right)^{K+1}\left[1+\left(\frac{1+K}{1+\langle n\rangle}\right)e^{-t/\tau_c}\right]. \tag{30}$$

Comparing this result to Eq. (21), we see that $\bar{R}_K(t)$ has the same basic features as the unclipped correlation function $\bar{R}(l\Delta t)$, namely, a dc background term and a signal term.

We will now compute the ensemble-average statistical error on R_K for the following model of a clipped correlator. Features (i), (ii), (iii), and (iv) used in describing the ideal correlator in Sec. III will also be assumed here. At time $t = 0$ the correlator starts sampling the output from the photomultiplier with gates of duration $\delta t \le \Delta t$ where Δt is the time spacing between gates. The first gate in which the number of collected photocounts is larger than K triggers an N-channel multichannel scaler which records sequentially the number of counts obtained during the N gates immediately following the trigger. After the train of N gates, the multichannel scaler is reset to the first channel and is ready to be activated by the next trigger. This will occur when n again exceeds K. In each one of the N channels the new number of counts is added to the previous total. After $\mathfrak{M}_0$ triggers the lth channel contains the sum of all counts registered in all the $\mathfrak{M}_0$ gates occurring $l\Delta t$ after a trigger. The measured correlation function is then

$$R_{Kl} = \frac{1}{\mathfrak{M}_0}\sum_{m=1}^{\mathfrak{M}_0} n^{(K)}(t_m)n(t_m + l\Delta t) , \tag{31}$$

with $\bar{R}_{Kl}$ given by Eq. (30) with $t = l\Delta t$. The mean-square statistical error on R_{Kl} has the form

$$\langle \delta R_{Kl}{}^2\rangle = \frac{1}{\mathfrak{M}_0^2}\sum_{j=1}^{\mathfrak{M}_0}\sum_{m=1}^{\mathfrak{M}_0}\langle n^{(K)}(t_j)n(t_j + l\Delta t)n^{(K)} \times (t_m)n(t_m + l\Delta t)\rangle - \bar{R}_{Kl}{}^2 . \tag{32}$$

We assume that the number of channels is large enough such that $N\Delta t > 2\tau_c$; in this case it is a good approximation to say that counts related to two different triggers $j \neq k$ are uncorrelated, that is,

$$\langle n_j^{(K)} n_{j+l}\, n^{(K)}{}_m n_{m+l}\rangle = \langle n_j^{(K)} n_{j+l}\rangle \langle n_m^{(K)} n_{m+l}\rangle \quad (33)$$

for $j \neq m$. In Eq. (33) we have introduced the abbreviated notation

$$n_j^{(K)} \equiv n^{(K)}(j\Delta t) \text{ and } n_{j+l} = n(t_j + l\Delta t) . \quad (34)$$

Using Eq. (34) we have for $\langle \delta R_{Kl}{}^2\rangle$

$$\langle \delta R_{Kl}{}^2\rangle = \frac{\langle n_j^{(K)2} n_{j+l}{}^2\rangle - \bar{R}_{Kl}{}^2}{\mathfrak{M}_0} . \quad (35)$$

The problem is now to evaluate the average appearing on the right-hand side of Eq. (35). This can be done quite easily by using the two-dimensional generating function Q_2

$$Q_2(s_1, s_2) = \langle (1-s_1)^{n_1}(1-s_2)^{n_2}\rangle . \quad (36)$$

Utilizing the properties of Q_2 given in Sec. II, one finds

$$\langle n_j^{(K)2} n_{j+l}{}^2\rangle = \langle n^2\rangle + \sum_{m=0}^{K} \frac{(-1)^m}{m!}\left(\frac{\partial^m}{\partial s_2^m}\frac{\partial^2}{\partial s_1^2} Q_2(s_1 - 1, s_2)\right)\Big|_{s_1=s_2=1} . \quad (37)$$

From Eqs. (30), (35), and (37) we obtain

$$\langle \delta R_{Kl}{}^2\rangle = \frac{\langle n\rangle^2}{\mathfrak{M}_0}\Big\{ 2 + 4A - 2B + C - x^{2K+2} - \left[4A - 2B + 2C + 2\left(\frac{(1+K)}{1+\langle n\rangle}\right)x^{2K+2}\right]e^{-l\Delta t/\tau_c} + \left[A + C - \left(\frac{1+K}{1+\langle n\rangle}\right)^2 x^{2K+2}\right]e^{-2l\Delta t/\tau_c}\Big\} + \frac{\langle n\rangle}{M_0} , \quad (38)$$

with

$$x = \langle n\rangle/(1+\langle n\rangle) \quad (39)$$

and

$$\begin{aligned} A &= 2 - (K+2)(K+3)x^{K+1} + 2(K+1)(K+3)x^{K+2} - (K+1)(K+2)x^{K+3} , \\ B &= 2 - (K+1)(K+2)x^{K} + 2K(K+2)x^{K+1} - K(K+1)x^{K+2} , \\ C &= 2 - K(K+1)x^{K-1} + 2(K-1)(K+1)x^{K} - K(K-1)x^{K+1} . \end{aligned} \quad (40)$$

Once again a preliminary indication of the accuracy of the measured correlation function is the ratio of the root-mean-square error $\langle \delta R_{Kl}{}^2\rangle^{1/2}$ to the amplitude of the exponential signal part of R_{Kl} in the limit $l \to 0$,

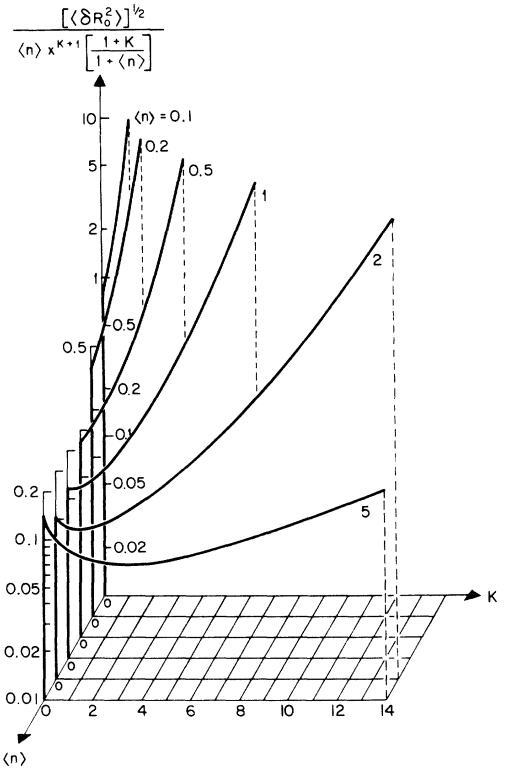

FIG. 3. rms fractional error Δ_K for the clipped correlator model versus counting rate and clipping level.

$$\Delta_K = \frac{\langle \delta R_{K0}{}^2\rangle^{1/2}}{\langle n\rangle x^{K+1}(1+K)/(1+\langle n\rangle)} . \quad (41)$$

The relative statistical error Δ_K for our clipped correlator model can be most meaningfully contrasted with Δ_R for the ideal correlator model of Sec. III if we compare results obtained for an equal total measurement time T rather than for an equal number of samples $\mathfrak{M}_0 = M_0$. For the ideal correlator we had simply $M_0 = T/\Delta t$. For the clipped correlator we are dealing with there is no possibility of a new trigger for a time $N\Delta t$ following any given trigger. Furthermore after the series of N gates is completed there will also be a waiting time before the next trigger. If W is the average waiting time in units of Δt then the total number of triggers in the time T is

$$\mathfrak{M}_0 = T/(N+W)\Delta t . \quad (42)$$

It can be shown that W is simply the reciprocal of the probability of finding $n > K$ in one interval δt; that is,

$$W = \left(\frac{1+\langle n\rangle}{\langle n\rangle}\right)^{K+1} . \quad (43)$$

Figure 3 shows the dependence of Δ_K on $\langle n\rangle$ and K calculated with $T = 10$ sec, $\tau_c = 10^{-3}$ sec, $\delta t = \Delta t$

$= 0.03\,\tau_c$, and $N = 100$. We note first that for moderate values of $\langle n\rangle$ there is a minimum in the error as a function of the clipping level K. This minimum is a consequence of two competing factors; as K increases, the error on a single sample of R_{Kl} *decreases*; however, increasing K also decreases the number of samples $\mathfrak{N}_0$ as seen via Eqs. (42) and (43). We see that for $\langle n\rangle \leq 1$ the value of K which minimizes the error is $K = 0$. In the limit of large $\langle n\rangle$ the optimum K is $K \cong 0.76\,\langle n\rangle$.

In Fig. 2 we give Δ_K explicitly as a function of $\langle n\rangle$ choosing for each $\langle n\rangle$ the optimum value of K. The asymptotic behavior of Δ_K in the two limits $\langle n\rangle \to 0$ and $\langle n\rangle \to \infty$ can be evaluated easily from Eq. (38). For large $\langle n\rangle$ we have $\langle \delta R_{K0}{}^2\rangle \propto \langle n\rangle^2$; Δ_K becomes independent of $\langle n\rangle$ and equal to

$$\Delta_K = 4.34[(N+2.14)\Delta t/T]^{1/2}\,, \quad \langle n\rangle \to \infty \tag{44}$$

where $K = 0.76\,\langle n\rangle$ and $W = 2.14\Delta t$ is the average waiting time for optimum K. The ratio $T/(N+2.14) \times \Delta t$ is just the number of independent samples of R_{Kl}. If we recall that our basic assumptions demand that $(N+2.14)\Delta t \gtrsim 2\tau_c$ in order to maintain statistical independence of all samples, we have

$$\Delta_K \gtrsim 6.14(\tau_c/T)^{1/2}\,, \quad \langle n\rangle \to \infty\,. \tag{45}$$

This result can be compared with the corresponding asymptotic expression for the ideal correlator as given in Eq. (25).

In the limit $\langle n\rangle \to 0$, Eq. (38) gives

$$\langle \delta R_{K0}{}^2\rangle = \langle n\rangle/\mathfrak{N}_0 \cong \Delta t/T\,, \quad \langle n\rangle \to 0 \tag{46}$$

and Eq. (30) gives for the amplitude of the signal part of R_K, $R_{K0}(\text{signal}) = \langle n\rangle^2$, from which we find

$$\Delta_K = \left(\frac{\Delta t}{T}\right)^{1/2} \frac{1}{\langle n\rangle^2}\,, \quad \langle n\rangle \to 0\,. \tag{47}$$

This behavior of Δ_K versus $\langle n\rangle$ is quite different from that obtained for the ideal correlator, cf. Eq. (27) and Fig. 2; in particular $\langle \delta R_0{}^2\rangle$ is in the present case independent of $\langle n\rangle$ rather than decreasing linearly with $\langle n\rangle$. Equation (46) can be understood intuitively by noting that each measurement of R_{K0} is a product $n^{(K)}n = (1)\times(n)$; therefore, the variance on an individual sample is just $\langle n\rangle$. However the number of samples is not constant as it was for the ideal correlator model, but decreases linearly with $\langle n\rangle$ as $\langle n\rangle \to 0$.

V. STATISTICAL ERRORS ON THE MEASURED CORRELATION TIME

The most important information contained in a measurement of the decaying exponential type correlation function that we have been considering is the correlation time τ. Once R_l is measured, with $l = 0, 1, 2, \ldots, N$, τ can be determined by a least-mean-squares fitting procedure to the appropriate functional form. We now derive the relation between the mean-square error in τ and the mean-square errors in the R_l and R_{Kl} corresponding to our two correlator models. In each case we carry out a generalized procedure in which the measured correlation function is fitted to the function

$$R_l = B + Ae^{-lH}\,, \tag{48}$$

where $H \equiv \Delta t/\tau$. We consider first the ideal digital correlator model of Sec. III. Our fit in this case is found by seeking the minimum value of the function f defined as

$$f(A, B, H) = \sum_{l=0}^{N} (B + Ae^{-lH} - R_l)^2\,, \tag{49}$$

where $N\Delta t$ is the maximum delay for which we compute R_l so that N represents the number of "channels" of simultaneous measurement of the correlation function. From the usual conditions for a minimum in f, $\partial f/\partial A = 0$, $\partial f/\partial B = 0$, and $\partial f/\partial H = 0$, we obtain a set of three equations in the three unknown quantities A, B, and H. The equations are linear in A and B; therefore, by substitution we can eliminate A and B to obtain a single equation in H. That equation is

$$C_{\mathrm{I}} \sum_{l=0}^{N} R_l + C_{\mathrm{II}} \sum_{l=0}^{N} R_l e^{-lH} + \sum_{l=0}^{N} lR_l e^{-lH} = 0\,, \tag{50}$$

where

$$C_{\mathrm{I}} = \left(\frac{\partial D_1}{\partial H}\right)\frac{D_2}{(N+1)D_2 - D_1^2} - \left(\frac{\partial D_2}{\partial H}\right)\frac{D_1}{2[(N+1)D_2 - D_1^2]}\,, \tag{51}$$

$$C_{\mathrm{II}} = \frac{N+1}{2}\left(\frac{\partial D_2}{\partial H}\right)\frac{1}{(N+1)D_2 - D_1^2} - \left(\frac{\partial D_1}{\partial H}\right)\frac{D_1}{(N+1)D_2 - D_1^2}\,,$$

and

$$D_1 = \frac{1 - e^{-(N+1)H}}{1 - e^{-H}}\,, \quad D_2 = \frac{1 - e^{-2(N+1)H}}{1 - e^{-2H}}\,. \tag{52}$$

Without computing an explicit solution for H from Eq. (50) for a given measured set of R_l we can determine the effect of a change in the R_l on H by differentiating Eq. (50) viewed as a function of H and the R_l. The result is

$$-\sum_{l=0}^{N} (\delta R_l)(C_{\mathrm{I}} + C_{\mathrm{II}}e^{-lH} + le^{-lH}) = (\delta H)\sum_{l=0}^{N} R_l\left(\frac{\partial C_{\mathrm{I}}}{\partial H} + \frac{\partial C_{\mathrm{II}}}{\partial H}e^{-lH} - lC_{\mathrm{II}}e^{-lH} - l^2e^{-lH}\right). \tag{53}$$

Assuming that the $\delta R_l (l = 0, 1, \ldots, N)$ are now the differences between the measured and the true ensemble-average correlation function and are all statistically independent, we square and ensemble-average Eq. (53) to obtain

$$\langle \delta H^2\rangle = \frac{1}{F^2}\sum_{l=0}^{N} C_l^2 \langle \delta R_l{}^2\rangle\,, \tag{54}$$

where

$$C_l = \bar{C}_I + \bar{C}_{II} e^{-l\bar{H}} + l e^{-l\bar{H}} \tag{55}$$

and

$$F = \langle n\rangle^2 \Bigg((N+1)\frac{\partial \bar{C}_I}{\partial \bar{H}} + \bar{D}_1 \frac{\partial \bar{C}_I}{\partial \bar{H}} + \bar{D}_2 \frac{\partial \bar{C}_{II}}{\partial \bar{H}} + \bar{C}_{II}\frac{\partial \bar{D}_1}{\partial \bar{H}} + \tfrac{1}{2}\bar{C}_{II}\frac{\partial \bar{D}_2}{\partial \bar{H}} - \frac{\partial^2 \bar{D}_1}{\partial \bar{H}^2} - \frac{1}{4}\frac{\partial^2 \bar{D}_2}{\partial \bar{H}^2}\Bigg) . \tag{56}$$

The overbarred quantities, $\bar{C}_I$, $\bar{C}_{II}$, etc., are the result of replacing H by $\bar{H} = \Delta t/\tau_c$ in Eqs. (51) and (52). In calculating F we also made the substitution $R_l = \bar{R}_l = \langle n\rangle^2(1 + e^{-l\Delta t/\tau_c})$ in the right-hand side of Eq. (53). Replacing R_l and H by their ensemble average values has the effect of neglecting errors in H which are of second order in δR_l.

Finally then the root-mean-square fractional error in the measured correlation time τ is simply

$$\Delta_\tau \equiv \frac{\langle \delta\tau^2\rangle^{1/2}}{\tau_c} = \frac{\langle \delta H^2\rangle^{1/2}}{\bar{H}} = \frac{1}{F\bar{H}}\left(\sum_{l=0}^{N} C_l^2 \langle \delta R_l^2\rangle\right)^{1/2} , \tag{57}$$

where the $\langle \delta R_l^2\rangle$ are the ensemble-average statistical errors already computed in Sec. III.

A treatment identical to that given above can be used to obtain the error in τ for the clipped correlator model of Sec. IV. For this case the fractional error has the form

$$_K\Delta_\tau \equiv \frac{\langle \delta\tau^2\rangle^{1/2}}{\tau_c} = \frac{1}{F_K\bar{H}}\left(\sum_{l=0}^{N} C_l^2 \langle \delta R_{Kl}^2\rangle\right)^{1/2} , \tag{58}$$

with C_l given by Eq. (55) and

$$F_K = \langle n\rangle x^{K+1}\Bigg[(n+1)\frac{\partial \bar{C}_I}{\partial \bar{H}} + D_1 \frac{\partial \bar{C}_{II}}{\partial \bar{H}} + \bar{C}_{II}\frac{\partial \bar{D}_1}{\partial \bar{H}} - \frac{\partial^2 \bar{D}_1}{\partial \bar{H}^2} + \frac{1+K}{1+\langle n\rangle} \times\left(\bar{D}_1 \frac{\partial \bar{C}_I}{\partial \bar{H}} + \bar{D}_2 \frac{\partial \bar{C}_{II}}{\partial \bar{H}} - \tfrac{1}{2}\bar{C}_{II}\frac{\partial \bar{D}_2}{\partial \bar{H}} - \frac{1}{4}\frac{\partial^2 \bar{D}_2}{\partial \bar{H}^2}\right)\Bigg] . \tag{59}$$

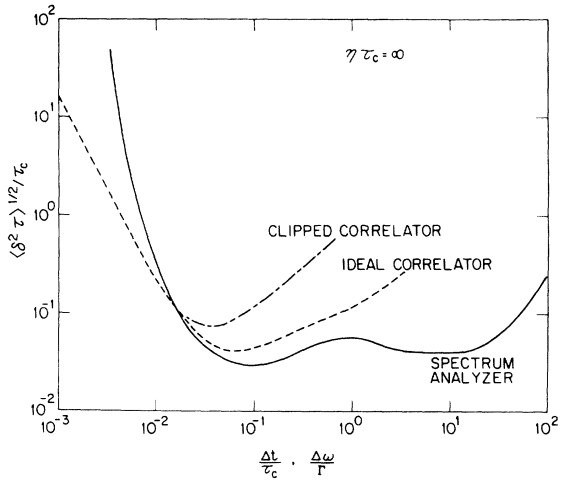

FIG. 4. rms fractional correlation-time error in the limit of infinite counting rate versus the "channel position" parameters $\Delta t/\tau_c$ and $\Delta\omega/\Gamma$.

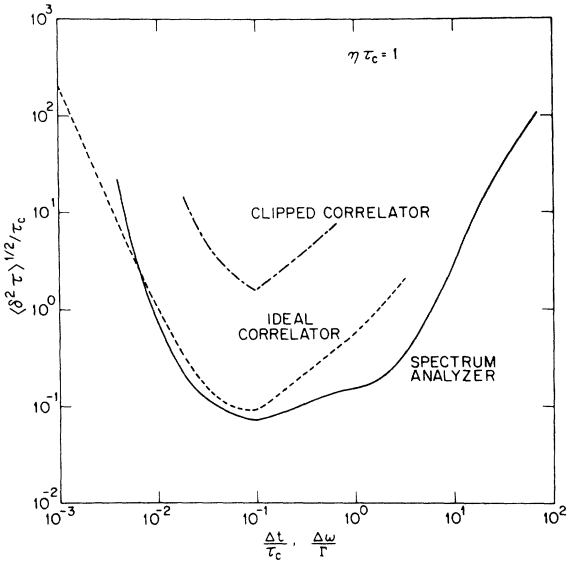

FIG. 5. rms fractional correlation-time error versus the "channel position" parameters $\Delta t/\tau_c$ and $\Delta\omega/\Gamma$ in the case $\eta\tau_c = 1$.

We now present a series of numerical computations of Δ_τ and $_K\Delta_\tau$ which were carried out in order to answer the following questions:

(a) What is the optimum time-delay placement for a given number of channels of computation of R_l or R_{Kl}, i.e., what is the value of $\Delta t/\tau_c$ that minimizes the correlation time error for fixed N?

(b) Does this optimum value of $\Delta t/\tau_c$ depend on the counting rate η?

(c) How do Δ_τ and $_K\Delta_\tau$ vary with $\langle n\rangle$—and K for the clipped correlator—for the best choice of $\Delta t/\tau_c$?

(d) What is the variation of the correlation time errors with a changing number of channels, N?

(e) How do the two correlator models compare in terms of their respective errors on τ_c when each is operated for the same period of time?

(f) How do these two correlation techniques compare with the more common spectrum-measurement approach to be described in Sec. VII?

Figures 4 and 5 show the variation of Δ_τ and $_K\Delta_\tau$ as a function of $\Delta t/\tau_c$ for two counting rates, $\eta\tau_c = \infty$ and $\eta\tau_c = 1$, respectively. The results were calculated assuming the following parameter values: $T = 10$ sec, $\tau_c = 10^{-3}$ sec, $\delta t = \Delta t$ except when $\Delta t > 0.1\tau_c$ in which case we set $\delta t = 0.1\tau_c$,[37,38] and $N = 100$ for both correlators. For the clipped correlator, K was adjusted to its optimum value for each $\Delta t/\tau_c$, that is, the value that gave the lowest error on τ_c.

One can see that in every case there is a mini-

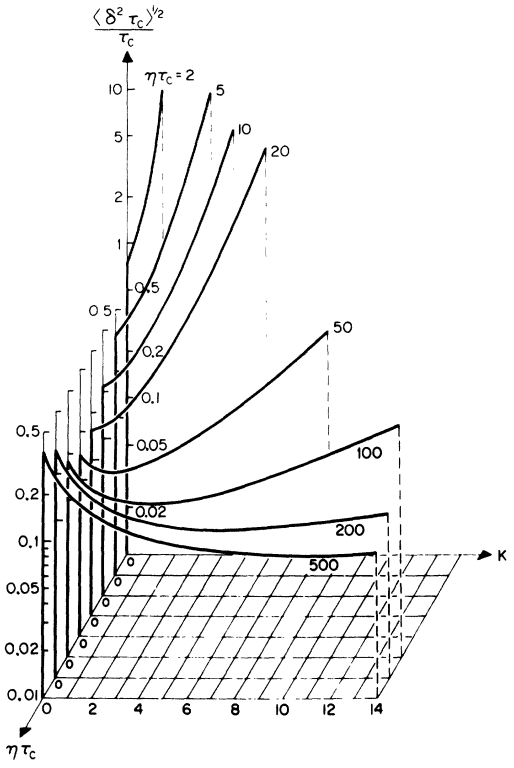

FIG. 6. rms correlation-time error for the clipped correlator model as a function of the counting rate per correlation time, $\eta\tau_c$, and the clipping level K.

mum in error versus $\Delta t/\tau_c$. Furthermore, the position of this minimum is only weakly dependent on counting rate. The existence of such a minimum is in essence the result of an interplay between three factors. As Δt increases from zero for fixed N, the N channels span a wider portion of the exponential signal part of the correlation function thus initially driving the error down. However the fractional error on R_l and R_{Kl} relative to the *signal part* becomes large at large delays, $l\Delta t \gg \tau_c$. Therefore as Δt increases beyond some critical value the channels at large delays, $N\Delta t \gg \tau_c$, contain no useful information on τ_c and the error increases. Third, small values of Δt are also detrimental because of the reduction in the number of counts per Δt which results in an increase of the fractional errors on the correlation function at low counting rates, $\eta\tau_c < 1$. This last effect is particularly significant for the clipped correlator as can be seen from Fig. 2.

In answer to question (c) posed above, we next consider the effect of the clipping level K on ${}_K\Delta_\tau$ for various values of $\langle n \rangle$. By choosing the same values of T and τ_c used in Figs. 4 and 5 and the value of $\Delta t/\tau_c$ which minimized the error for each $\langle n \rangle$, we computed the results shown in Fig. 6. Because the optimum $\Delta t/\tau_c$ is essentially constant for the entire range of K and $\langle n \rangle$, ${}_K\Delta_\tau$ is controlled primarily by the variation of the correlation function fractional error, Δ_K. Thus Fig. 6 is qualitatively very similar to Fig. 3. In particular, we again find that for each $\langle n \rangle$ there is in fact an optimum choice for K. For large values of $\langle n \rangle$ this optimum value is $K \cong 0.76\ \langle n \rangle$.

To answer the rest of question (c) we plot in Fig. 7 both Δ_τ and ${}_K\Delta_\tau$ versus $\langle n \rangle$ for the following choice of parameters: $T = 10$ sec, $\tau_c = 10^{-3}$ sec; $\Delta t/\tau_c$ is the optimum value for each $\langle n \rangle$; K is also taken to be its optimum value in every case. Again because $\Delta t/\tau_c$ is essentially constant the qualitative behavior of Δ_τ and ${}_K\Delta_\tau$ with $\langle n \rangle$ mirrors the behavior of Δ_R and Δ_K shown in Fig. 2.

It is useful to point out that the specific numerical results given in Fig. 7 may be scaled to arbitrary values of Δt, τ_c, and T. Our general expressions for Δ_τ and ${}_K\Delta_\tau$ are functions of T, τ_c, Δt, $\langle n \rangle$ and for the clipped correlator K. However, the values of Δt and K which minimize the error are implicitly determined by τ_c and $\langle n \rangle$, respectively. As a result one can show that functional forms of Δ_τ and ${}_K\Delta_\tau$ can be written as

$$\Delta_\tau = \frac{\varphi(\eta\tau_c)}{(T/\tau_c)^{1/2}}\ , \quad {}_K\Delta_\tau = \frac{\psi(\eta\tau_c)}{(T/\tau_c)^{1/2}}\ , \tag{60}$$

where $\varphi(\eta\tau_c)$ and $\psi(\eta\tau_c)$ are the functions which are presented graphically in Fig. 7. The usefulness of these scaling relationships is best illustrated by a simple example. Suppose we consider an experiment in which we will measure the intensity correlation time with a 100-channel ideal correlator. Further, suppose that we have $\tau_c \cong 10^{-6}$ sec and a counting rate $\eta\tau_c \cong 1$. Figure 7 predicts an error of 10% in τ_c for $\eta\tau_c = 1$ and $T/\tau_c = 10^4$. If we wish to measure τ_c to 1% accuracy, then we demand that $T/\tau_c = 10^6$. This corresponds to a 1-sec total measuring time. By the same scaling procedure the clipped correlator requires about 4 min to obtain τ_c to the same accuracy.

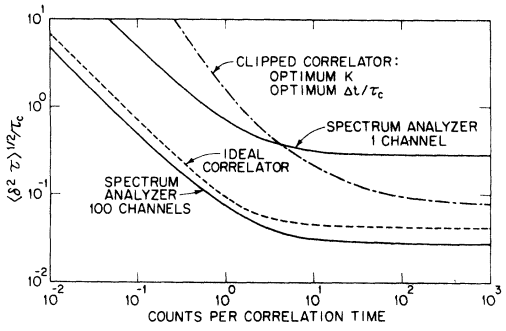

FIG. 7. rms fractional errors Δ_τ, ${}_K\Delta_\tau$, and Δ_Γ versus the counting rate per correlation time with all free parameters optimized.

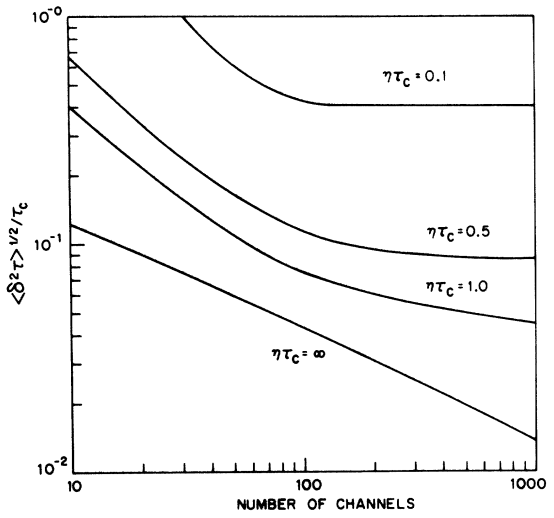

FIG. 8. Correlation-time error for the ideal correlator model versus the number of data channels and for various values of the counting rate.

Finally in Fig. 8 we give calculated values of Δ_τ for the ideal correlator model as a function of the number of measurement channels N. Each channel represents a measurement of R_l for a delay $l\Delta t$ in the range $0 \le l\Delta t \le N\Delta t$. For each value of N we computed Δ_τ as a function of $\Delta t/\tau_c$ to determine the optimum delay positions of the N channels. The result is that the error on τ is a minimum when the Nth channel corresponds to a delay $N\Delta t \cong 5\tau_c$. This result is not surprising if we note that there is little useful information on the exponential part of R_l for delays greater than $5\tau_c$. The optimum value of $\Delta t/\tau_c$ for any N is then approximately

$$(\Delta t/\tau_c)_{\text{optimum}} \cong 5/N \ . \tag{61}$$

For very large counting rates the error is a monotonic decreasing function of N. Over the range we investigated, $10 \le N \le 1000$, Δ_τ behaves approximately as $1/\sqrt{N}$. However, for counting rates in the range $\eta\tau_c \cong 1$, Δ_τ levels off at a minimum as N increases. This saturation can be explained by noting that as we put an increasing number of channels into the range of delay times between zero and $5\tau_c$ there is a corresponding decrease in the number of available counts per channel, $\langle n \rangle$. As $\langle n \rangle$ decreases the error on R_l increases, finally offsetting the effect of the increasing number of measurement points.

VI. STATISTICAL ERRORS IN MEASUREMENT OF PHOTOCURRENT SPECTRUM

We now deal with the statistical errors present in a determination of the intensity time evolution of an optical field as obtained by an optical mixing "self-beat" or "homodyne" spectrometer.[10] This technique involves measuring the power spectral density rather than the correlation function of the photocurrent. Using the fact that this power spectral density $S(\omega)$ is the Fourier transform of $G^{(2)}(t)$, we obtain the general features of $S(\omega)$ shown in Fig. 9. Comparing Figs. 1 and 9 we find that $S(\omega)$ consists of three contributions: a signal term $i_S^2(\omega)$, which mirrors the intensity power spectral density; a uniform background $i_N^2(\omega)$, which is the shot-noise term associated with the average photocurrent; and a δ function at $\omega = 0$ whose area is simply the square of the time-average photocurrent.

Our model apparatus to measure $S(\omega)$ is shown in block diagram form in Fig. 10. The important features of this device can be summarized as follows. The time-varying current output of a photodetector is passed through a narrow-band electronic filter having a center frequency ω_0 and a bandwidth $\Delta\omega_f$. The transfer function for this filter is shown inset in Fig. 10. The filtered current signal, consisting now of frequencies in the range $\omega_0 - \frac{1}{2}\Delta\omega_f \le \omega \le \omega_0 + \frac{1}{2}\Delta\omega_f$, is then rectified by a square-law detector. The output of this detector consists of two parts, a dc signal proportional to the total time-average *power* passing through the filter and a fluctuating noise signal arising from nonlinear mixing between the various frequency components which are present at the square-law detector input. This interfering noise has a triangularly shaped spectrum which is peaked at $\omega = 0$ and goes to zero at $\omega = 2\Delta\omega_f$. Finally the dc part of the detector output is isolated by a low pass filter (integrator) whose bandwidth satisfies the inequality $\Delta\omega_T \ll 2\Delta\omega_f$. Clearly in the usual case in which $\Delta\omega_f$ is small compared to the spectral width of the features of the photocurrent signal the resultant filtered output is proportional to current power spectral density at the frequency ω_0, $S(\omega_0)$.

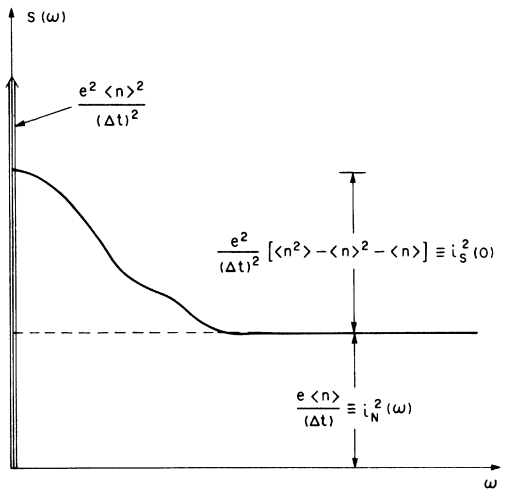

FIG. 9. General features of the photocurrent power spectral density.

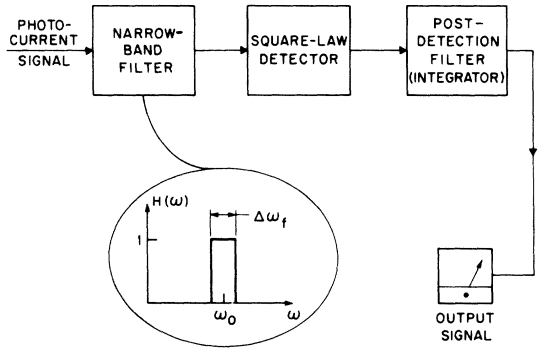

FIG. 10. Simplified block diagram of one data channel of a "self-beat" photocurrent spectrometer.

To make our error analysis considerations analogous to those used for the ideal and clipped correlator models we make the following assumptions for the measurement of $S(\omega)$. The power spectral density is measured simultaneously at $N+1$ frequencies given by $\omega_l = l\Delta\omega$, where l is integral and runs from zero to N and $\Delta\omega \geq \Delta\omega_f$. This requires $N+1$ data channels identical to that shown in Fig. 9. We now determine the ensemble-average mean-square errors $\langle \delta S^2(\omega) \rangle$ on the measured $S(\omega)$ for this proposed model.

Under the assumption that the photocurrent may be regarded as a quasicontinuous random function the operation of the self-beat spectrometer can be analyzed using classical electrical-engineering concepts. Since these calculations are well documented,[1,2,4,15,26] we merely quote those results that are necessary in our analysis. Following the notation used in Fig. 9, we find

$$\langle \delta S^2(\omega) \rangle = \frac{\pi}{\Delta\omega_f T} \bar{S}(\omega)^2 = \frac{\pi}{\Delta\omega_f T} [\langle i_S^2(\omega) \rangle + \langle i_N^2(\omega) \rangle]^2 , \tag{62}$$

where $\bar{S}(\omega)$ is the ensemble-average power spectral density and T is the response time of the postdetection filter, which we assumed to be a simple RC filter with a time constant $T = RC$. Thus T gives the total measurement time used to obtain the set of $N+1$ values of $S(\omega_l)$.

An important preliminary indication of the accuracy of the measured $S(\omega_l)$ is the ratio of rms uncertainty on $S(\omega_l)$ to the value of the signal term $\langle i_S^2(\omega) \rangle$. From Eq. (62) we have immediately

$$\frac{\langle \delta S^2(\omega) \rangle^{1/2}}{\langle i_S^2(\omega) \rangle} = \left(\frac{\pi}{\Delta\omega_f T} \right)^{1/2} \frac{\langle i_S^2(\omega) \rangle + \langle i_N^2(\omega) \rangle}{\langle i_S^2(\omega) \rangle} . \tag{63}$$

We now evaluate this ratio explicitly assuming a Gaussian optical field with an exponentially decaying intensity correlation function, e^{-t/τ_c}. In this case the ensemble-average photocurrent spectrum has the form

$$\bar{S}(\omega) = \langle i_S^2(\omega) \rangle + \langle i_N^2(\omega) \rangle = \frac{Z_1}{1 + \omega^2/\Gamma^2} + Z_2 , \tag{64}$$

where $\Gamma \equiv 1/\tau_c$ and Z_1 and Z_2 are constants involving the correlation time, the photocount rate, and the electronic charge e. The signal part of the spectrum is a Lorentzian centered at zero frequency with a half-width at half-height, Γ. The ratio $Z_1/Z_2 = \langle i_S^2(0) \rangle / \langle i_N^2(0) \rangle$, sometimes called the predetection signal-to-noise ratio, is given by

$$(S/N)_{\text{PRE}} = Z_1/Z_2 = \eta\tau_c , \tag{65}$$

where η is the photocounting rate *per coherence area*. From Eqs. (63)–(65) we find the fractional uncertainty in $S(\omega)$ at $\omega = 0$ as[39]

$$\Delta_S \equiv \frac{\langle \delta S^2(0) \rangle^{1/2}}{\langle i_S^2(0) \rangle} = \left(\frac{\pi}{\Delta\omega_f T} \right)^{1/2} \left(1 + \frac{1}{\eta\tau_c} \right) . \tag{66}$$

The ratio Δ_S is analogous to the ratios Δ_R and Δ_K computed for the two correlator models. Figure 2 shows the behavior of Δ_s as a function of $\eta\tau_c$ for the following choice of experimental parameters: $T = 10$ sec, $\tau_c = 10^{-3}$ sec, and $\Delta\omega_f = 0.1\Gamma$.

In the limit of high counting rate, $\eta\tau_c \to \infty$, Δ_s becomes independent of $\eta\tau_c$ and has the value

$$\Delta_S = (\pi/\Delta\omega_f T)^{1/2} , \quad \eta\tau_c \to \infty . \tag{67}$$

Since we have assumed the condition $\Delta\omega_f \ll \Gamma$, the response time of the analyzing filter, τ_f, satisfies the inequality $\tau_f \gg \tau_c$; therefore, $(\pi/\Delta\omega_f T)^{-1}$ is the number of statistically independent samples of $S(0)$ obtained in the time T. Note that the filter response time rather than the correlation time limits the independent sampling rate.

In the limit $\eta\tau_c \to 0$ we find from Eq. (66)

$$\Delta_S = \left(\frac{\pi}{\Delta\omega_f T} \right)^{1/2} \frac{1}{\eta\tau_c} , \quad \eta\tau_c \to 0 . \tag{68}$$

This can again be cast into the form of one over the square root of the number of independent samples by noting that only a fraction $(\eta\tau_c)^2$ of the total number of samples contains any information on $S(\omega)$ in the limit $\eta\tau_c \to 0$.

As was the case for the correlator-model results, the asymptotic error expressions, Eqs. (67) and (68), allow the numerical data of Fig. 2 to be scaled to arbitrary choices for the experimental parameters T, τ_c, and $\Delta\omega_f$.

We now proceed to determine the statistical errors on the measured linewidth of $S(\omega)$. Once $S(\omega)$ has been obtained at the $N+1$ frequencies $l\Delta\omega$, $0 \leq l \leq N$, Γ can be determined by a least-mean-squares fitting procedure to the proper functional form. Using the same generalized fitting procedure employed in Sec. V, we can calculate the mean square error in Γ from the known statistical errors on the $S(\omega_l)$. We assume for the fitting function the form suggested by Eq. (64),

$$\bar{S}(l\Delta\omega)=\bar{S}_l=A'/(1+l^2G^2)+B' , \tag{69}$$

where $G\equiv\Delta\omega/\gamma$ and γ is the best-fit half-width. Abbreviating the notation on the set of measured spectrum points to $S_l\equiv S(\omega=l\Delta\omega)$, we look for the minimum value of the function defined by

$$f'(A', B', G)=\sum_{l=0}\left(B'+\frac{A'}{1+l^2G^2}-S_l\right)^2 . \tag{70}$$

From the usual conditions $\partial f'/\partial A'=\partial f'/\partial G=\partial f'/\partial B'=0$ one obtains a set of three equations in the three unknowns A', B', and G. By substitution one can eliminate the linear parameters A' and B' and obtain a single equation in G; this equation is

$$C_{\mathrm{I}}'\sum_{l=0}^{N}S_l+C_{\mathrm{II}}'\sum_{l=0}^{N}\frac{S_l}{1+l^2G^2}\sum_{l=0}^{N}\frac{S_l}{(1+l^2G^2)^2}=0 , \tag{71}$$

where

$$C_{\mathrm{I}}'=\frac{Y_2^2-Y_1Y_3}{Y_2(N+1)-Y_1^2} , \quad C_{\mathrm{II}}'=\frac{Y_3(N+1)-Y_1Y_2}{Y_2(N+1)-Y_1^2} , \tag{72}$$

and

$$Y_K=\sum_{l=0}^{N}\frac{1}{(1+l^2G^2)^K} . \tag{73}$$

Without computing an explicit solution for G from Eq. (71) for a given set of measured S_l, we can determine the effect of a change in S_l on G by differentiating that equation considered as a function of G and S_l. The result is

$$\sum_{l=0}^{N}\delta S_l\left(\frac{1}{(1+l^2G^2)^2}-\frac{C_{\mathrm{II}}'}{(1+l^2G^2)}-C_{\mathrm{I}}'\right)$$
$$=\delta G\sum_{l=0}^{N}S_l\left(\frac{\partial C_{\mathrm{I}}'}{\partial G}+\frac{1}{1+l^2G^2}\frac{\partial C_{\mathrm{II}}'}{\partial G}-2C_{\mathrm{II}}'\frac{l^2G}{(1+l^2G^2)^2}+4\frac{l^2G}{(1+l^2G^2)^3}\right) . \tag{74}$$

Now allowing the δS_l to be the statistical differences between the measured and the true ensemble-average spectrum and assuming that the δS_l are all statistically independent, we obtain by squaring and then ensemble-averaging Eq. (74)

$$\langle\delta G^2\rangle=\frac{1}{(F')^2}\sum_{l=0}^{N}(C_l')^2\langle\delta S_l^2\rangle , \tag{75}$$

with

$$C_l'=\bar{C}_{\mathrm{I}}'+\frac{\bar{C}_{\mathrm{II}}}{1+l^2\bar{G}^2}-\frac{1}{1+l^2\bar{G}^2} \tag{76}$$

and

$$F'=\frac{\partial\bar{C}_{\mathrm{I}}'}{\partial\bar{G}}\left(\bar{Y}_1+\frac{N+1}{\eta\tau_c}\right)+\frac{\partial\bar{C}_{\mathrm{II}}'}{\partial\bar{G}}\left(\bar{Y}_2+\frac{\bar{Y}_1}{\eta\tau_c}\right)-\frac{2\bar{C}_{\mathrm{II}}'}{\bar{G}}$$
$$\times\left((\bar{Y}_2-\bar{Y}_3)+\frac{\bar{Y}_1-\bar{Y}_2}{\eta\tau_c}\right)+\frac{4}{\bar{G}}\left((\bar{Y}_3-\bar{Y}_4)+\frac{\bar{Y}_2-\bar{Y}_3}{\eta\tau_c}\right) . \tag{77}$$

The overbarred quantities, $\bar{C}_{\mathrm{I}}'$, $\bar{C}_{\mathrm{II}}'$, etc., are the result of replacing G by $\bar{G}=\Delta\omega/\Gamma=(\Delta\omega)\tau_c$ in Eqs. (71), (72), and (73). In calculating F' we also made the substitution $S_l=\bar{S}_l$ in the right-hand side of Eq. (74). Replacing S_l and G by their ensemble-average values has the effect of neglecting errors in G which are of second order in δS_l. Finally then the fractional error in Γ is

$$\Delta_\Gamma=\frac{\langle\delta\Gamma^2\rangle^{1/2}}{\Gamma}=\frac{\langle\delta G^2\rangle^{1/2}}{\bar{G}}=\frac{1}{F'\bar{G}}\left(\sum_{l=0}^{N}(C_l')^2\langle\delta S_l^2\rangle\right)^{1/2} . \tag{78}$$

We now present a series of numerical computations of Δ_Γ which were carried out in order to answer the following questions:

(i) What is the optimum frequency placement of a given number of equally spaced channels of measurement of S_l; i.e., what is the optimum value of $\Delta\omega/\Gamma$ for given N?

(ii) Does this optimum value of $\Delta\omega/\Gamma$ depend on the predetection signal-to-noise ratio $(S/N)_{\mathrm{PRE}}=\eta\tau_c$?

(iii) How does the linewidth error Δ_Γ vary with $\eta\tau_c$ for this optimum $\Delta\omega/\Gamma$.

(iv) How does Δ_Γ for the light mixing spectrometer compare to the correlation time errors Δ_τ and ${}_K\Delta_\tau$ calculated in Sec. III.

Figures 4 and 5 show the variation of Δ_Γ as a function of $\Delta\omega/\Gamma$ for $\eta\tau_c=\infty$ and $\eta\tau_c=1$, respectively. These results were obtained with parameter values of $T=10$ sec, $1/\Gamma=\tau_c=10^{-3}$ sec, and $\Delta\omega_f=\Delta\omega$ except when $\Delta\omega>0.1\Gamma$, in which case we set $\Delta\omega_f=(0.1)\Gamma$. The number of channels was taken as $N=100$.

One can see that in each case there is a minimum in the error versus $\Delta\omega/\Gamma$. The position of this minimum is insensitive to the value of $\eta\tau_c$ and occurs at $\Delta\omega/\Gamma\cong 0.1$. The existence of an optimum $\Delta\omega/\Gamma$ can be explained qualitatively as follows. Consider the case $\eta\tau_c<1$ first. As $\Delta\omega/\Gamma$ increases from zero for fixed N, the N data channels span a wider portion of the Lorentzian part of the spectrum thus initially driving the error down. However, the fractional error on S_l relative to the signal part becomes large at high frequencies, $l\Delta\omega\gg\Gamma$ if $\eta\tau_c<1$. Therefore as $\Delta\omega$ increases beyond some critical value the channels at high frequencies contain no useful information on Γ and the error increases. Small values of $\Delta\omega/\Gamma$ are also unfavorable since the fractional error on S_l is proportional to $(\Delta\omega_f T)^{-1}=[(\Delta\omega)T]^{-1}$. For $\eta\tau_c\gg 1$ the first and third arguments given above are still valid. Now, however, the fractional error on S_l relative to the signal term is a constant independent of frequency [cf. Eq. (63)]. But in the limit $\eta\tau_c\to\infty$ the ensemble-average spectrum becomes

$$\bar{S}_l=Z_1/[1+(l\Delta\omega/\Gamma)^2] . \tag{79}$$

Therefore measurements at frequencies $l\Delta\omega\gg\Gamma$

determine only the product $Z_1\Gamma^2$. So here again the error on Γ must increase as $\Delta\omega/\Gamma$ becomes large; now, however, because there are fewer data channels near $\Delta\omega/\Gamma \sim 1$ to provide information on Z_1 and Γ separately. That this is a very weak effect can be seen in the shallowness of the minimum in Δ_Γ for $\eta\tau_c = \infty$.

Finally in Fig. 7 we plot Δ_Γ versus $\eta\tau_c$ for the usual choice of parameters: $T = 10$ sec, $\tau_c = 1/\Gamma = 10^{-3}$ sec, $N = 100$ channels. The ratio $\Delta\omega/\Gamma$ was taken as its optimum value for each $\eta\tau_c$. Since this optimum value is nearly constant, the qualitative behavior of Δ_Γ with $\eta\tau_c$ is determined by the variation of Δ_s with $\eta\tau_c$ and can be explained by reference to Eqs. (67) and (68).

We again note that the specific numerical results of Fig. 7 may be scaled to arbitrary values of Γ, $\Delta\omega$, and T. Our general result for Δ_Γ is a function of T, Γ, $\Delta\omega$, and $\eta\tau_c$. However, the value of $\Delta\omega$ which minimizes the linewidth error is implicitly determined by Γ and $\eta\tau_c$. As a result Δ_Γ may be written in the functional form

$$\Delta_\Gamma = \frac{\sigma(\eta\tau_c)}{(T/\tau_c)^{1/2}} , \tag{80}$$

where $\sigma(\eta\tau_c)$ is the function given graphically in Fig. 7. This curve may then be used to determine the linewidth error for arbitrary counting rate, correlation time, and measurement time.

VII. EFFECT OF OPTICAL FIELD SPATIAL INCOHERENCE

In all the calculations presented so far in this paper we have assumed that the photodetector is illuminated by a spatially coherent (single electromagnetic mode) optical field. A simple analysis shows that gathering light from many spatial coherence areas of the field has a markedly different effect on a photocurrent correlation function measurement as compared to an optical mixing spectrum determination.

In a situation where the photodetector views more than a single region of spatial coherence let us divide up the photosurface into smaller areas inside of which the optical field may be taken as spatially coherent. Then the total photocurrent can be written as

$$i(t) = \sum_{\alpha=1}^{c} i_\alpha(t) , \tag{81}$$

where c is the number of coherence areas and $i_\alpha(t)$ is the photocurrent from the αth coherence area. We choose the size of our coherence area such that the photocurrents generated in two different areas may be taken as uncorrelated. With this assumption we write

$$\langle i_\alpha(t_1) i_\beta(t_2)\rangle = \langle i_\alpha\rangle\langle i_\beta\rangle \tag{82}$$

for $\alpha \neq \beta$. Letting the average current $\langle i_\alpha\rangle$ be the same for all α, we have the correlation function for the total photocurrent as

$$\langle i(t_1) i(t_2)\rangle = \sum_{\alpha=1}^{c}\sum_{\beta=1}^{c} \langle i_\alpha(t_1) i_\beta(t_2)\rangle$$
$$= c\langle i_\alpha(t_1) i_\alpha(t_2)\rangle + c(c-1)\langle i_\alpha\rangle^2 . \tag{83}$$

Subtracting off the average dc current term from $\langle i_\alpha(t_1) i_\alpha(t_2)\rangle$ and defining $R_\alpha(t_1, t_2)$ as the current correlation function for the shot-noise and signal parts of $\langle i_\alpha(t_1) i_\alpha(t_2)\rangle$ yields

$$\langle i(t_1) i(t_2)\rangle = cR_\alpha(t_1, t_2) + c^2\langle i_\alpha\rangle^2 . \tag{84}$$

Equation (84) indicates that the shot-noise and signal contributions to the total correlation function both grow linearly with c while the dc current term increases as c^2.

Now Eq. (63) shows that the fractional rms error on the current spectrum measured at frequency ω is determined completely by the ratio of the shot-noise to signal powers $i_N^2(\omega)/i_S^2(\omega)$. Since $i_N^2(\omega)$ and $i_S^2(\omega)$ are, respectively, the shot-noise and signal components of the Fourier time transform of $cR_\alpha(t_1, t_2)$, both increase linearly with c. Therefore the statistical errors associated with a current spectrum measurement are independent of c and determined only by the counting rate per correlation time *per coherence area*, $\eta\tau_c$.[1,2,4,15,26]

On the other hand, in a measurement of the current correlation function the statistical error is related to the ratio of the error in the dc plus signal parts to the signal-term amplitude. Since the dc term increases as c^2 while the signal term is linear in c, we expect that the error on the correlation function will increase with c. Returning to the ideal correlator model of Sec. III, we can explicitly determine the dependence of $\langle \delta R_l^2\rangle$ on c as follows.

The measured correlation function [cf. Eq. (15)] is now

$$R_l = \frac{1}{M_0}\sum_{j=1}^{M_0} n_j n_{j+l} , \tag{85}$$

where n_j is the total number of counts recorded in the interval δt at $t = j\Delta t$. The statistics of the process n_j are, in general, quite complicated for $c \neq 1$ and must be determined from a knowledge of the mutual coherence function of the optical field. Such a calculation has recently been carried out by Jakeman and Pike[40] for a specific light scattering and light collection geometry. In order to simplify the problem, while retaining all the essential features of the general calculation, we will assume that the output of the photodetector represents the superposition of c statistically independent contributions from c different coherence areas in the optical field. We take the individual c contributions to have the same statistical properties, namely, a Bose-

Einstein single-time ensemble distribution, an average number of counts $\langle n\rangle$ in the interval δt, and a correlation function $R(t)=\langle n\rangle^2(1+e^{-t/\tau_c})$. With these assumptions we write n_j as

$$n_j=\sum_{\alpha=1}^{c}{}_\alpha n_j\ , \tag{86}$$

where ${}_\alpha n_j$ is the number of counts produced in the αth coherence area. To calculate the errors on R_l we need the distribution functions $W_1(n;c)$, $W_2(n_1,n_2;c)$, etc., for the process n_j in terms of the known distributions for ${}_\alpha n_j$ that were given in Sec. II. For example, given the assumed statistical independence of ${}_\alpha n_j$ and ${}_\beta n_j$ for $\alpha\neq\beta$ we have[41]

$$W_1(n;c)=\sum_{n_1=0}^{\infty}\cdots\sum_{n_c=0}^{\infty}W_1\Big(n-\sum_{\alpha=1,\,\alpha\neq1}^{c}n_\alpha\Big)\,W_1\Big(n-\sum_{\alpha=1,\,\alpha\neq2}^{c}n_\alpha\Big)\cdots W_1\Big(n-\sum_{\alpha=1,\,\alpha\neq c}^{c}n_\alpha\Big)$$

$$=\sum_{n_1=0}^{c}\cdots\sum_{n_c=0}^{c}W_1(n_1)\cdots W_1(n_c)\delta_{n-n_1-n_2-\cdots-n_c}\ . \tag{87}$$

Thus $W_1(n;c)$ is the c-fold convolution of the single coherence area distribution $W_1(n)$. It is easy to show that all the probability distributions $W_1(n;c)$, $W_2(n_1,n_2;c)$, etc., can in fact be represented as convolutions of the c identical distributions corresponding to a single coherence area. In this case the generating functions of the over-all distributions take on a particularly simple form

$$Q_m(s_1,s_2,\cdots,s_m;c)=Q_m^c(s_1,s_2,\cdots,s_m)\ . \tag{88}$$

Thus it is possible to easily compute any of the generalized moments for the counting process n_j using the known generating functions for $c=1$; for example, the ensemble-average correlation function becomes

$$\bar{R}(l\Delta t;c)=M_{11}(0,l;c)=c\langle n\rangle^2(c+e^{-l\Delta t/\tau_c})\ . \tag{89}$$

The mean-square error on R_l is a straightforward generalization of Eq. (18),

$$\langle\delta R^2(l;c)\rangle=\frac{M_{22}(0,l;c)}{M_0}+\frac{2(M_0-l)}{M_0^2}M_{121}(0,l,2l;c)$$

$$+\frac{2}{M_0^2}\sum_{s=1,\,s\neq l}^{M_0}(M_0-s)M_{1111}(0,l,s+l;c)-M_{11}^2(0,l;c)\ . \tag{90}$$

A straightforward evaluation of the various general moments yields

$$\begin{aligned}
&M_{11}=F_{11}=c\langle n\rangle^2(c+e^{-l\Delta t/\tau_c})\ ,\\
&F_{22}=F_{21}=c(c+1)\langle n\rangle^3(c+2e^{-l\Delta t/\tau_c})\ ,\\
&F_{22}=c(c+1)\langle n\rangle^4[c(c+1)+4(c+1)e^{-l\Delta t/\tau_c}+2e^{-2l\Delta t/\tau_c}]\ ,\\
&M_{22}=F_{22}+2F_{12}+M_{11}\ ,\\
&F_{111}=c\langle n\rangle^3[c^2+2ce^{-l\Delta t/\tau_c}+(c+2)e^{-2l\Delta t/\tau_c}]\ ,\\
&F_{121}=c(c+1)\langle n\rangle^4[c^2+4ce^{-l\Delta t/\tau_c}+(c+6)e^{-2l\Delta t/\tau_c}]\ ,\\
&M_{121}=F_{121}+M_{111}\ ,\\
&M_{1111}(s>l)=c\langle n\rangle^4[c^3+2c^2e^{-l\Delta t/\tau_c}+2c(c+2)e^{-s\Delta t/\tau_c}\\
&\qquad+ce^{-2l\Delta t/\tau_c}+2(c+1)e^{-2s\Delta t/\tau_c}\\
&\qquad+(c+2)^2e^{-(s+l)\Delta t/\tau_c}+c^2e^{-(s-l)\Delta t/\tau_c}]\ ,
\end{aligned} \tag{91}$$

from which we find

$$\begin{aligned}
\langle\delta R^2(l;c)\rangle=&\frac{1}{M_0}\Big\{\langle n\rangle^4\Big[-4c^3-c^2+\frac{8c^3}{1+e^{-\Delta t/\tau_c}}+\frac{2c^2}{1-e^{-2\Delta t/\tau_c}}+e^{-2l\Delta/\tau_c}\Big(8c^2l-4c(c+2)+\frac{8c(2c+1)}{1-e^{-\Delta t/\tau_c}}\Big)+e^{-4l\Delta t/\tau_c}\\
&\times\Big(2c(c+2)l-c(c+2)+\frac{2c(c+2)}{1-e^{-2\Delta t/\tau_c}}\Big)\Big]+\langle n\rangle^3[2c^2(2c+1)+4c(2c+1)e^{-l\Delta t/\tau_c}+2c(c+2)e^{-2l\Delta t/\tau_c}]\\
&+\langle n\rangle^2(c^2+ce^{-l\Delta t/\tau_c})\Big\}
\end{aligned} \tag{92}$$

and in the limit $l\to0$

$$\langle\delta R^2(0,c)\rangle=\frac{1}{M_0}\Big[\langle n\rangle^4\Big(-4c^3-6c^2-2c-8+\frac{8(c^3+2c^2+c)}{1-e^{-\Delta t/\tau_c}}+\frac{4(c^2+c)}{1-e^{-2\Delta t/\tau_c}}\Big)+\langle n\rangle^3(4c^3+12c^2+8c)+\langle n\rangle^2(c^2+c)\Big]\ . \tag{93}$$

In all of these results $\langle n\rangle$ is the average number of counts in the interval δt per single coherence area. For $c=1$ these expressions reduce to those derived in Sec. III.

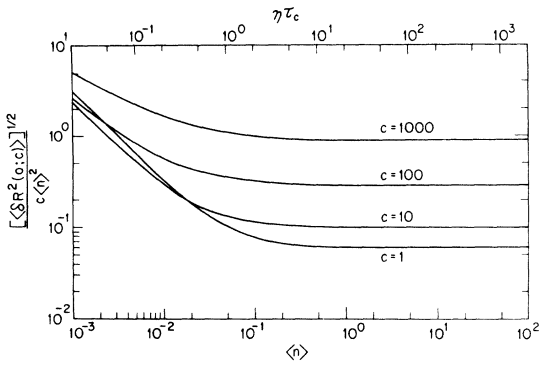

FIG. 11. Correlation-function fractional error for the ideal correlator model versus counting rate and the number of coherence areas c.

We may again take as a significant indication of the accuracy of the measurement of R_l the ratio of the rms error as $l \to 0$ to the signal-term amplitude, namely,

$$\Delta_R(c) = \langle \delta R^2(0;\, c) \rangle^{1/2} / c\langle n\rangle^2 \,. \tag{94}$$

Figure 11 shows the calculated variation of $\Delta_R(c)$ versus counting rate for various values of c and the following parameter values: $T = 10$ sec, $\tau_c = 10^{-3}$ sec, $\Delta t/\tau_c = 0.05$. At high counting rates, $\langle n\rangle > 1$, $\Delta_R(c)$ is strongly c dependent; e.g., the situation $c = 1000$ results in a 16-fold increase in rms error compared to the result for $c = 1$. In the limits $\langle n\rangle \to \infty$ and $c \to \infty$ we have approximately

$$\Delta_R(c) \cong (8c\tau_c/T)^{1/2}, \quad \langle n\rangle \to \infty, \quad c \to \infty \,. \tag{95}$$

This asymptotic expression may be compared to Eq. (25) which is correct for $\langle n\rangle \to \infty$ and $c = 1$.

A calculation of the statistical error on the measured correlation time τ for $c \neq 1$ is straightforward. Using Eqs. (89) and (92) for $\bar{R}(l\Delta t;\, c)$ and $\langle \delta R^2(l;\, c)\rangle$ in the generalized least-mean-squares fitting procedure given in Sec. V, we find [cf. Eq. (57)]

$$\Delta_\tau(c) \equiv \frac{\langle \delta^2\tau\rangle^{1/2}}{\tau_c} = \frac{\langle \delta H^2\rangle^{1/2}}{\bar{H}}$$

$$= \left(\sum_{l=0}^{N} C_l^2 \langle \delta R^2(l;\, c)\rangle \right)^{1/2} \Big/ F(c)\bar{H} \,, \tag{96}$$

where the coefficients C_l are identical to those defined in Eq. (55) and where

$$F(c) = \langle n\rangle^2 \left[c^2 \left((N+1)\frac{\partial \bar{C}_I}{\partial \bar{H}} + \bar{D}_1 \frac{\partial \bar{C}_{II}}{\partial \bar{H}} + \bar{C}_{II}\frac{\partial \bar{D}_1}{\partial \bar{H}} - \frac{\partial^2 \bar{D}_1}{\partial \bar{H}_2} \right) \right.$$

$$\left. + c\left(\bar{D}_1 \frac{\partial \bar{C}_I}{\partial \bar{H}} + \bar{D}_2 \frac{\partial \bar{C}_{II}}{\partial \bar{H}} + \tfrac{1}{2}\bar{C}_{II}\frac{\partial \bar{D}_2}{\partial \bar{H}} - \frac{1}{4}\frac{\partial^2 \bar{D}_2}{\partial \bar{H}^2} \right) \right] \tag{97}$$

in the same notation used in Sec. V.

Numerical calculations of $\Delta_\tau(c)$ for c in the range $1 \leq c \leq 1000$ and with $N = 100$ showed that increasing the number of coherence areas had no effect on the optimum time-delay placement of the N data channels. In every case the lowest value of $\Delta_\tau(c)$ corresponded to the choice $N\Delta t \cong 5\tau_c$. Figure 12 shows the calculated variation of $\Delta_\tau(c)$ versus the average counting rate per coherence area per Δt for the same choice of parameters used to obtain Fig. 7. The adverse effect of collecting light from a large number of coherence areas is clearly evident.

VIII. DISCUSSION

We have carried out an analysis of the statistical errors on the optical-intensity correlation function as measured by two photocounting digital-correlator models and on the intensity spectrum as measured by a "self-beating" optical-mixing spectrometer. From these errors and a generalized least-mean-squares fitting procedure we have determined the uncertainty on the measured correlation time (linewidth) for the case of a Gaussian optical field with an exponential intensity correlation function (a Lorentzian spectrum). Scaling relationships have been given which permit our numerical results to be applied to an arbitrary set of experimental parameters.

In order to make a comparison between the various experimental methods we have dealt with, it is useful to refer to the results given in Figs. 7, 8, and 12. We see that in the case of a single coherence area field the fractional errors on τ for the 100-channel ideal correlator are quite comparable to the errors on Γ for the 100-channel spectrum analyzer at all counting rates. From a practical point of view, however, 100 simultaneous channels of spectrum analysis capable of operating in real time and flexible enough to tolerate a large range in measured half-widths represents an unrealistically complicated solution to the problem in the present state of the art. On the other hand, it might appear that a 100-channel ideal correlator operating in

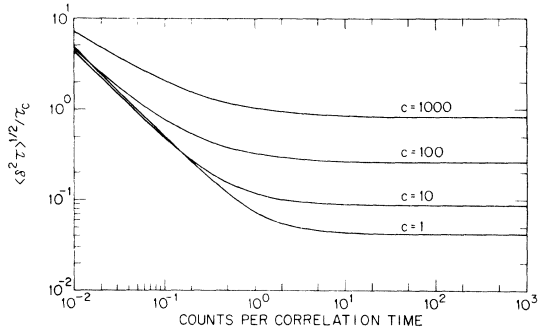

FIG. 12. rms correlation-time error for the ideal correlator model versus counting rate and the number of coherence areas c with all other parameters optimized.

real time would be limited to long-correlation-time measurements because of the necessity of performing the multiplications $n_j n_{j+l}$ from which the correlation function is computed. However, Fig. 7 indicates that with only a small sacrifice in accuracy on τ_c we may operate such a device at a counting rate such that $\eta\tau_c \cong 1$. In the latter case we would find $n_j = 0$, 1 with small probability of $n_j = 2$; the required multiplications can be done by simple coincidence. It would thus appear quite feasible to construct such a device, using state-of-the-art digital techniques, which would be useful for all τ_c greater than about 10^{-8} sec. Being an all digital instrument, there is no device-limited upper bound on the correlation times which such a correlator could measure.

The clipped correlator avoids the $n_j n_{j+l}$ multiplication problem via its "0" or "1" quantization of n_j. From Fig. 7 we see that the 100-channel clipped correlator can be quite competitive with the ideal correlator at very large counting rates but that the rapidly increasing error with decreasing $\langle n \rangle$ soon makes this device even less attractive than the usual *single* channel of spectrum analysis. However it should be noted that our clipped correlator model represents a very practical, easily built device and is not necessarily the most efficient model that can be devised using the concept of clipping.

In particular our model does not compute all possible photocount products $n_j(K)n_{j+l}$ on a real-time basis. If it did, then for counting rates such that $n_j = 0$ or 1 with only a small probability for $n_j = 2$ the clipped correlator with $K = 0$ would be essentially equivalent to our ideal correlator model.

Another practical consideration in our comparison is the effect of gathering light from an increasing number of spatial coherence areas of the optical field. In Sec. VIII we showed that the error on τ_c for the ideal correlator model increases for large c as $c^{1/2}$ while the error on Γ as derived from a spectrum measurement is independent of c. Therefore, in circumstances where it is desirable to collect light from a large number of coherence areas, for example, to overcome photodetector dark current, the N-channel spectrum analyzer is preferable to our model ideal correlator. This is *not* meant to imply that under such circumstances a measurement of the correlation function provides *intrinsically* less information than a comparable spectrum analysis experiment. It does imply that even our model "ideal" correlator does not make the most efficient possible use of the information present at the photodetector output. One can show, in fact, that by processing the photocurrent signal in a slightly different way one can obtain the signal part of the current autocorrelation function with an error which is essentially independent of the number of coherence areas.[42]

ACKNOWLEDGMENTS

The authors would like to acknowledge a number of helpful discussions with Professor F. T. Arecchi, Professor T. Greytak, and Professor S. R. Chen that took place during the course of this work. One of us (J. B. L.) is grateful to Bell Telephone Laboratories for the use of its facilities in preparing this paper for publication. We would also like to thank Professor G. B. Benedek for making this collaboration possible.

---

*Research supported in part by the Advanced Research Projects Agency under Contract No. SD-90.

†NATO-CNR Research Fellow. Permanent address: Laboratori CISE, Milano, Italy.

‡Present address: Bell Laboratories, Murray Hill, New Jersey 07974.

[1]A. T. Forrester, R. A. Gudmundsen, and P. O. Johnson, Phys. Rev. 99, 1691 (1955).

[2]A. T. Forrester, J. Opt. Soc. Am. 51, 253 (1961).

[3]G. B. Benedek, in *Polarization, Matter and Radiation*, edited by la Société Française de Physique (Presses Universitaire de France, Paris, 1969).

[4]H. Z. Cummins and H. L. Swinney, in *Progress in Optics*, edited by E. Wolf (North-Holland, Amsterdam, 1970), Vol. VIII.

[5]I. L. Fabelinskii, *The Molecular Scattering of Light*, translated by R. T. Beyer (Plenum, New York, 1968).

[6]B. Chu and F. J. Schoenes, Phys. Rev. Letters 21, 6 (1968); S. S. Alpert, Y. Yeh, and E. Lipworth, *ibid.* 14, 486 (1965).

[7]P. N. Pusey and W. I. Goldberg, Appl. Phys. Letters 13, 321 (1968).

[8]H. Z. Cummins, N. Knable, and Y. Yeh, Phys. Rev. Letters 12, 150 (1964); S. B. Dubin, J. H. Lunacek, and G. B. Benedek, Proc. Natl. Acad. Sci. U. S. 57, 1164 (1967).

[9]J. B. Lastovka and G. B. Benedek, Phys. Rev. Letters 17, 1039 (1966).

[10]N. C. Ford, Jr. and G. B. Benedek, Phys. Rev. Letters 15, 649 (1965).

[11]H. L. Swinney and H. Z. Cummins, Phys. Rev. 171, 152 (1968).

[12]M. A. Bouchiat and J. Meunier, Phys. Rev. Letters 23, 752 (1969).

[13]J. S. Huang and W. W. Webb, Phys. Rev. Letters 23, 160 (1969).

[14]Orsay Liquid Crystal Group, Phys. Rev. Letters 22, 1361 (1969).

[15]G. B. Benedek, in *Statistical Physics, Phase Transitions and Superfluidity*, edited by M. Chrétien, E. P. Gross, and S. Deser (Gordon and Breach, New York, 1968), Vol. II.

[16]C. Freed and H. A. Haus, Phys. Rev. 141, 287 (1966); J. A. Armstrong and A. W. Smith, in *Progress in Optics*, edited by E. Wolf (North-Holland, Amsterdam, 1967), Vol. VI, pp. 211–257.

[17]F. T. Arecchi, V. Degiorgio, and B. Querzola, Phys. Rev. Letters 19, 1168 (1967); F. Davidson and L. Man-

del, Phys. Letters 25A, 700 (1967); F. T. Arecchi, M. Giglio, and A. Sona, *ibid.* 25A, 341 (1967); M. Lax and M. Zwanziger, Phys. Rev. (to be published).

[18]D. B. Scarl, Phys. Rev. Letters 17, 663 (1966).

[19]D. T. Phillips, H. Kleiman, and S. P. Davis, Phys. Rev. 153, 113 (1967).

[20]R. Hanbury-Brown and R. Q. Twiss, Nature 177, 27 (1956); R. Q. Twiss, A. G. Little, and R. Hanbury-Brown, *ibid.* 180, 324 (1957).

[21]S. H. Chen and N. Polonsky-Ostrowsky, Opt. Commun. 1, 64 (1969); G. A. Rebka and R. V. Pound, Nature 180, 1035 (1957); B. L. Morgan and L. Mandel, Phys. Rev. Letters 16, 1012 (1966); W. Martienssen and E. Spiller, Am. J. Phys. 32, 919 (1964).

[22]F. T. Arecchi, A. Berné, and A. Sona, Phys. Rev. Letters 17, 260 (1966).

[23]F. T. Arecchi, E. Gatti, and A. Sona, Phys. Letters 20, 27 (1966).

[24]E. Jakeman, C. J. Oliver, and E. R. Pike, J. Phys. A 1, 406 (1968).

[25]F. T. Arecchi, A. Berné, A. Sona, and P. Burlamacchi, IEEE J. Quantum Electron. QE-2, 341 (1966); E. Jakeman and E. R. Pike, J. Phys. A 1, 690 (1968).

[26]J. B. Lastovka, Ph.D. thesis (Massachusetts Institute of Technology, 1967) (unpublished).

[27]M. G. Kendall and A. Stuart, *The Advanced Theory of Statistics* (Hafner, New York, 1966), Vol. III, Chap. 48; R. Zwanzig and N. K. Ailawadi, Phys. Rev. 182, 280 (1969).

[28]H. A. Haus, in *Quantum Optics, The Proceedings of the Enrico Fermi International School of Physics, Varenna*, edited by R. J. Glauber (Academic, New York, 1969).

[29]R. J. Glauber, in *Quantum Optics and Electronics*, edited by C. de Witt, A. Blandin, and C. Cohen-Tannoudji (Gordon and Breach, New York, 1964); L. Mandel and E. Wolf, Rev. Mod. Phys. 37, 231 (1965).

[30]F. Davidson and L. Mandel, Phys. Letters 27A, 579 (1968).

[31]G. Bédard, Phys. Rev. 161, 1304 (1967).

[32]A thorough discussion of the techniques which are useful in processing the photomultiplier output can be found in I. DeLotto, P. F. Manfredi, and P. Principi, Energia Nucl. (Milan) 11, 557 (1964); F. T. Arecchi, in Ref. 28; S. Fray, F. A. Johnson, R. Jones, T. P. McLean, and E. R. Pike, Phys. Rev. 153, 357 (1966).

[33]Similar considerations have been applied by Jakeman and Pike (Ref. 25) in discussing the errors on the factorial moments of a photocount distribution.

[34]An approximate form for Δ_R has been calculated by P. N. Pusey, J. Appl. Phys. (to be published).

[35]J. H. Van Vleck and D. Middleton, Proc. IEEE 54, 2 (1966).

[36]E. Jakeman and E. R. Pike, J. Phys. A 2, 411 (1969).

[37]We have not allowed δt to become greater than $0.1\tau_c$ in order to avoid two difficulties: (a) the Bose-Einstein from which we used for $W_1(n, \delta t)$ in Eq. (20) is valid only for $\delta t \ll \tau_c$; (b) in a situation where the inequality $\delta t \ll \tau_c$ is violated the measured correlation function in the limit $M_0 \to \infty$ is more rigorously the convolution of the true correlation function with the correlators instrumental response function; $H(t) = 1$ for $-\frac{1}{2}\delta t \leq t \leq \frac{1}{2}\delta t$ and $H(t) = 0$ otherwise. In the case $\delta t \lesssim \tau_c$ a deconvolution of the measured R_I or $R_{K,I}$ and $H(t)$ would be necessary prior to fitting to the functional form of Eq. (48).

[38]Very recently E. Jakeman, E. R. Pike, and S. Swain [J. Phys. A, 3, L55 (1970)] have given a preliminary report of an extension of our results involving a more exact form for the counting distributions that does not require the restriction $\delta t \ll \tau_c$.

[39]Actually Eq. (66) is rigorously the limit $\omega \to 0$ neglecting the δ-function contribution to $S(\omega)$ at $\omega = 0$.

[40]E. Jakeman, C. J. Oliver, and E. R. Pike, J. Phys. A 3, 145 (1970).

[41]L. Mandel, Proc. Phys. Soc. (London) 81, 1104 (1963).

[42]J. B. Lastovka and V. Degiorgio (to be published).

PHYSICAL REVIEW A VOLUME 4, NUMBER 5 NOVEMBER 1971

Brandow Boson Linked-Cluster Expansion Applied to the High-Density Charged Boson Gas*

J. C. Lee

Department of Physics, Northwestern State University of Louisiana, Natchitoches, Louisiana 71457

(Received 2 June 1971)

The Brandow boson linked-cluster expansion has been used to redo the Foldy calculation of the Bogoliubov theory for a charged boson gas. The particle-number conservation is treated exactly. The ring diagrams have been summed using the same techniques as used by Gell-Mann and Brueckner for the electron gas. The next-most-divergent diagrams (twisted rings) have also been summed. These diagrams contain a renormalized hole line and thus show explicitly the dynamics of the condensate which is treated only in an average way in the Bogoliubov theory. The results for the ground-state energy and the condensation fraction agree exactly with Foldy in the high-density limit.

While the Brueckner-Goldstone linked-cluster expansion[1] for the interacting fermion systems has found many successful applications in the past, there has been an obstacle to a direct application of this diagramatic perturbation theory to the interacting boson systems. The difficulty is due,